Spatial Regulation of ABCG25, an ABA Exporter, Is an Important Component of the Mechanism Controlling Cellular ABA Levels

Youngmin Park,[a] Zheng-Yi Xu,[b,1] Soo Youn Kim,[b,2] Jihyeong Lee,[a] Bongsoo Choi,[a] Juhun Lee,[a] Hyeran Kim,[c] Hee-Jung Sim,[c] and Inhwan Hwang[a,b,3]

[a] Division of Integrative Biosciences and Biotechnology, Pohang University of Science and Technology, Pohang 790-784, Korea
[b] Department of Life Sciences, Pohang University of Science and Technology, Pohang 790-784, Korea
[c] Center for Genome Engineering Institute for Basic Science, Yuseong-gu 305-811, Daejeon, South Korea

ORCID IDs: 0000-0001-8869-4200 (B.C.); 0000-0002-1388-1367 (I.H.)

The phytohormone abscisic acid (ABA) plays crucial roles in various physiological processes, including responses to abiotic stresses, in plants. Recently, multiple ABA transporters were identified. The loss-of-function and gain-of-function mutants of these transporters show altered ABA sensitivity and stomata regulation, highlighting the importance of ABA transporters in ABA-mediated processes. However, how the activity of these transporters is regulated remains elusive. Here, we show that spatial regulation of ATP BINDING CASETTE G25 (ABCG25), an ABA exporter, is an important mechanism controlling its activity. ABCG25, as a soluble green fluorescent protein (sGFP) fusion, was subject to posttranslational regulation via clathrin-dependent and adaptor protein complex-2-dependent endocytosis followed by trafficking to the vacuole. The levels of sGFP:ABCG25 at the plasma membrane (PM) were regulated by abiotic stresses and exogenously applied ABA; PM-localized sGFP:ABCG25 decreased under abiotic stress conditions via activation of endocytosis in an ABA-independent manner, but increased upon application of exogenous ABA via activation of recycling from early endosomes in an ABA-dependent manner. Based on these findings, we propose that the spatial regulation of ABCG25 is an important component of the mechanism by which plants fine-tune cellular ABA levels according to cellular and environmental conditions.

INTRODUCTION

As sessile organisms, plants have to adjust their cellular processes constantly and dynamically according to ever-changing environmental conditions. The phytohormone abscisic acid (ABA) plays crucial roles in responses to abiotic and biotic stresses (Wilkinson and Davies, 2002; Zeevaart and Creelman, 1998; Zhu, 2002). ABA suppresses premature seed germination and regulates key plant growth and development processes, such as proper root architecture formation and lateral root development (De Smet et al., 2003; Duan et al., 2013). To elicit cellular responses, the ABA levels are rapidly elevated and then returned to lower levels after the responses (Seiler et al., 2011).

The ABA levels in plants are determined by two opposing processes, ABA biosynthesis and catabolism. Two biosynthetic pathways, de novo biosynthesis and hydrolysis of glucose from glucose-conjugated ABA (ABA-GE), increase the cellular ABA levels (Cheng et al., 2002; Dietz et al., 2000; Endo et al., 2008; Lee et al., 2006; Xu et al., 2012). The enzymes involved in de novo ABA

biosynthesis have been identified and characterized at the molecular level (Nambara and Marion-Poll, 2005). Except for the last two steps of the de novo ABA biosynthesis pathway, which occur in the cytosol, de novo ABA biosynthesis takes place in chloroplasts (Iuchi et al., 2000; Qin and Zeevaart, 1999; Tan et al., 2001, 2003). In addition, two ABA-GE-hydrolyzing enzymes, AtBG1 and AtBG2, have been identified in *Arabidopsis thaliana* (Lee et al., 2006; Xu et al., 2012). AtBG1 and AtBG2 localize to the endoplasmic reticulum (ER) and vacuole, respectively. Thus, ABA is produced at multiple subcellular locations. The biosynthetic pathways that produce ABA are activated under abiotic stress conditions. ABA catabolism is also mediated via multiple pathways. For instance, active ABA is converted to inactive ABA-GE via glucose conjugation. ABA UDP-glucosyltransferases (ABA-UGTs) mediate the conjugation reaction in the cytosol (Dong et al., 2014). The other pathway is hydroxylation of ABA to 8′- or 7′-hydroxyl ABA in the cytosol by members of the CYTOCHROME P450 FAMILY 707 SUBFAMILY A family. Hydroxylated ABA is spontaneously converted to phaseic acid and then to dihydrophaseic acid via soluble phaseic acid-reducing enzymes (Gillard and Walton, 1976). Upon rehydration after dehydration stress, the expression levels of *ABA-UGTs* and *CYP707A* genes are elevated to reduce the cellular ABA levels, whereas the expression levels of genes involved in ABA biosynthetic pathways are downregulated.

Another level of regulation in ABA homeostasis is transport of ABA across the plasma membrane (PM). Two ABA transporters have been identified in Arabidopsis (Kang et al., 2010; Kuromori et al., 2010), namely, ABCG25 and ABCG40, which function as an

ABA exporter and importer, respectively, and belong to the large family of ATP binding cassette (ABC) transporters and the subfamily ABCG in Arabidopsis. ABA-transporting activity was tested using heterologous systems such as yeast or regenerated membrane vesicles. Both transporters have a high affinity for (+)-ABA. Both loss-of-function and gain-of-function mutants of ABCG25 and ABCG40 display abnormal ABA sensitivity in seed germination and stomatal regulation. These results showed that these ABA transporters play important roles in ABA-mediated processes. However, how these proteins are regulated at the cellular levels under various developmental and environmental conditions remains elusive.

The activity of transporters localized to the PM is subject to regulation at multiple levels depending on the cellular and environmental conditions. One such level is transcriptional regulation and another is posttranslational regulation. Endocytosis is a key mechanism by which the abundance and/or turnover of PM proteins are regulated at the cellular level (Luschnig and Vert, 2014). Indeed, endocytosis plays a pivotal role in the polar distribution of proteins such as PIN-FORMEDs (PINs), auxin efflux carriers, and BOR1 (Boron transporter 1) (Dhonukshe et al., 2007; Takano et al., 2005). However, it remains unknown whether ABA transporters are subject to such regulation according to the growth and environmental conditions.

In this study, we examined how the ABA exporter ABCG25 is regulated at the posttranslational level under various environmental conditions. We provide evidence that, under abiotic stress conditions, ABCG25 levels at the PM decreased via enhanced clathrin-mediated endocytosis and vacuolar trafficking through the endosomal compartments. By contrast, application of exogenous ABA increased PM-localized ABCG25 levels via enhanced recycling to the PM from endosomes. Moreover, we show that endocytosis and enhanced recycling of a soluble green fluorescent protein fusion of ABCG25 (sGFP:ABCG25) occur in an ABA-independent and ABA-dependent manner, respectively.

RESULTS

sGFP:ABCG25 Localizes to the PM, Prevacuolar Compartment, and Lytic Vacuole

ABCG25 functions as an exporter of ABA and its overexpression leads to lowering of cellular ABA levels during germination (Kuromori et al., 2010). Thus, regulation of its activity would constitute an important mechanism by which plant cells control cellular ABA levels. To elucidate how the activity of ABCG25 is regulated at the cellular level, we generated transgenic Arabidopsis plants expressing soluble green fluorescent protein (sGFP)-fused ABCG25 (sGFP:ABCG25 plants). The native promoter of ABCG25 did not show any signals. Thus, we used the CaMV 35S promoter to express sGFP:ABCG25. sGFP:ABCG25 was readily detected at ~95 kD, the expected size of the chimeric protein, by immunoblot analysis using an anti-GFP antibody (Figure 1A). In addition, sGFP:ABCG25 plants exhibited the ABA-insensitive phenotype in the presence of 1 μM ABA during germination (Figure 1B), as observed upon overexpression of nontagged ABCG25 (Kuromori et al., 2010), confirming that the N-terminal sGFP moiety does not affect the activity of ABCG25.

Initially, we examined the localization of sGFP:ABCG25. It produced a prominent PM pattern as reported previously (Kuromori et al., 2010). In addition, sGFP:ABCG25 produced a clear punctate staining pattern (Figure 1C).

To define the identity of the organelle to which sGFP:ABCG25 localizes to give the punctate staining pattern, root tissues of the transgenic plants were stained with FM4-64, a lipophilic dye that is used as a tracer of endocytosis and localizes to various endosomal compartments as well as the PM (Meckel et al., 2004; Ueda et al., 2001). We examined the colocalization of FM4-64 with sGFP:ABCG25. FM4-64 initially stains the PM and then multiple endosomal compartments, the trans-Golgi network (TGN)/early endosome (EE), and the prevacuolar compartment (PVC), on its way from the PM to the lytic vacuole after endocytosis from the PM in a time-dependent manner. sGFP:ABCG25 partially colocalized with FM4-64 at the punctate labeling at 5 min after staining with FM4-64 (Figure 1C). To confirm the endosomal localization of sGFP:ABCG25, sGFP:ABCG25 seedlings stained with FM4-64 were treated with brefeldin A (BFA) and the localization of sGFP:ABCG25 was examined. Both sGFP:ABCG25 and FM4-64 localized to the BFA body (Figure 1D). To test if the punctate staining pattern of sGFP:ABCG25 is derived from newly synthesized proteins, we examined their colocalization after treatment with cycloheximide (CHX), a protein biosynthesis inhibitor. sGFP:ABCG25 still produced the punctate staining pattern and partially colocalized with FM4-64 at the punctate labeling at 5 min after FM4-64 staining (Figure 1E), indicating that the punctate staining pattern is not caused by newly synthesized sGFP:ABCG25 on its way to the PM.

The localization of sGFP:ABCG25 at multiple endosomes prompted us to examine whether sGFP:ABCG25 is transported to the lytic vacuole. To test this idea, we treated root tissues of sGFP:ABCG25 plants with Concanamycin A (Con A) and examined whether sGFP:ABCG25 is detected in the vacuole. Con A inhibits the vacuolar H^+-ATPase, thereby inhibiting protein degradation in the vacuole. Upon Con A treatment, the signal of sGFP:ABCG25 in the vacuole was significantly increased (Figure 1F). To avoid any side effects of the chemical treatment, sGFP:ABCG25 seedlings were incubated in the dark. Vacuole-localized proteins are more stable in the dark (Kleine-Vehn et al., 2008). The sGFP:ABCG25 signal intensity in the lytic vacuole was increased upon incubation for 6 h in the dark (Figure 1G), confirming that sGFP:ABCG25 is targeted to the lytic vacuole.

To define the identity of the sGFP:ABCG25-positive endosomal compartment, we crossed sGFP:ABCG25 plants with transgenic plants expressing VHA-a1:RFP, a TGN/EE marker, or ARA7:RFP, a PVC marker. Their localizations were examined in homozygous plants. sGFP:ABCG25 did not overlap with VHA-a1:RFP (Figures 2A and 2B). By contrast, sGFP:ABCG25 closely overlapped with ARA7:RFP, indicating that sGFP:ABCG25 localizes to the PVC (Figures 2C and 2D). The expression of sGFP:ABCG25 was driven by the strong constitutive CaMV 35S promoter. The high level of ABCG25 expression may change cellular ABA levels, which in turn may alter the localization of organellar markers, VHA-a1:RFP and ARA7:RFP. To eliminate this possibility, we treated root tissues of sGFP:ABCG25 plants with Wortmannin, an inhibitor of phosphatidylinositol-3-kinase. Wortmannin inhibits vesicle generation within the PVC in plants, thereby causing enlargement of PVCs
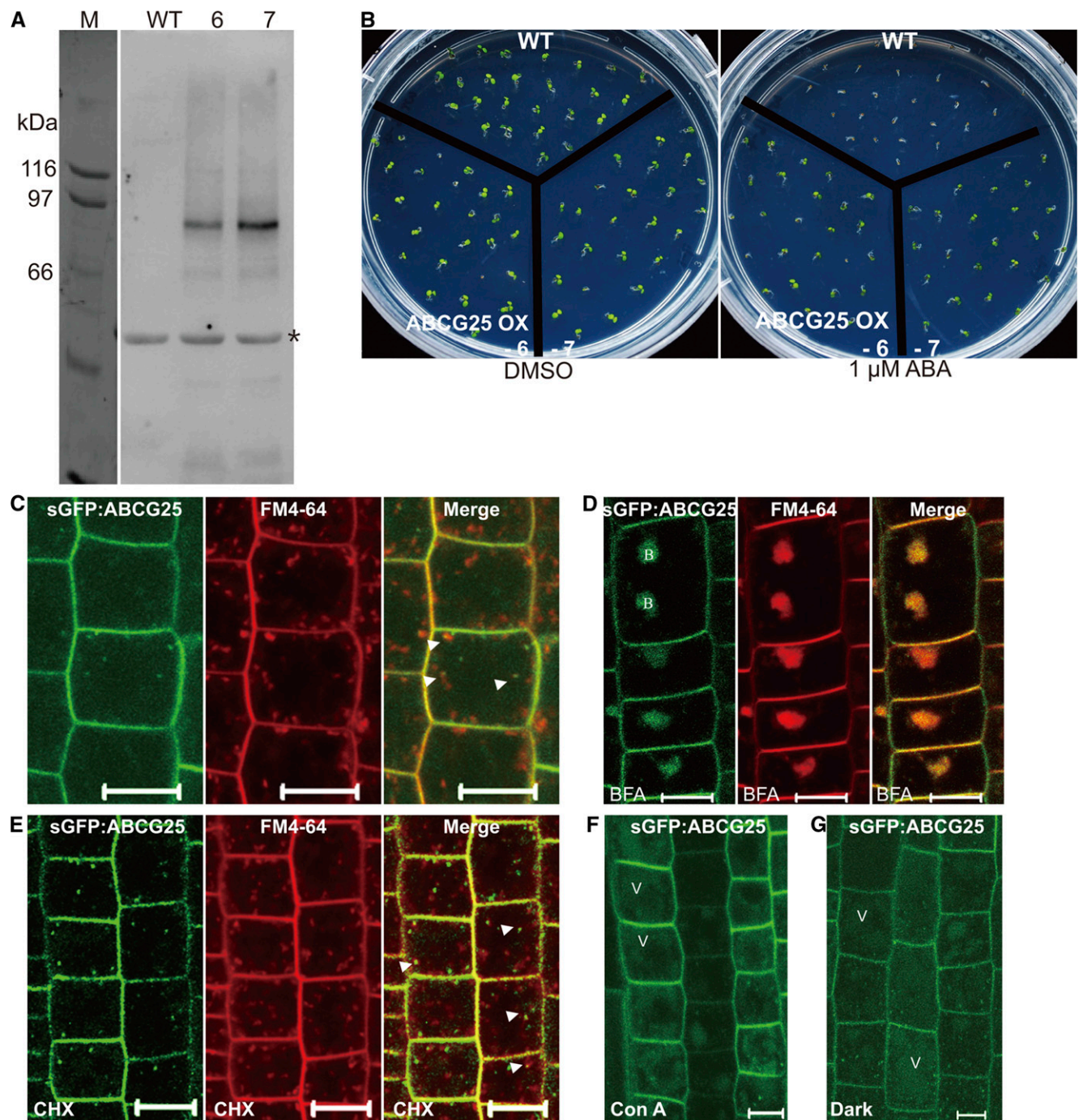
Figure 1. sGFP:ABCG25 Localizes to Various Subcellular Compartments in Transgenic Plants.

(A) Expression of *sGFP:ABCG25* in transgenic plants. Protein extracts were prepared from two independent transgenic lines (nos. 6 and 7) and analyzed by protein gel blotting using an anti-GFP antibody. Asterisk indicates nonspecific bands detected by the antibody.

(B) Functionality of sGFP:ABCG25. Wild-type and sGFP:ABCG25 plants of two independent lines were grown on 0.5× MS plates containing DMSO or 1 μM ABA. Images were taken 6 d after planting.

(C) to **(E)** Localizations of sGFP:ABCG25 and FM4-64. Five-day-old seedlings expressing *sGFP:ABCG25* were treated with FM4-64. The localizations of sGFP:ABCG25 and FM4-64 in root tip cells were examined 5 min after FM4-64 staining using CLSM **(C)**. Additionally, seedlings were treated with 50 μM BFA for 30 min **(D)** or with 50 μM CHX for 1 h **(E)**. Arrowheads indicate the merge between sGFP:ABCG25 and FM4-64. B, BFA body; V, vacuole. Green, sGFP: ABCG25; red, FM4-64; merge, overlay between sGFP:ABCG25 and FM4-64. Bars = 10 μm.

(Kleine-Vehn et al., 2008). sGFP:ABCG25-positive puncta were enlarged upon Wortmannin treatment (Figure 2E), confirming its localization to the PVC. The localization of sGFP:ABCG25 was further confirmed in *mag1-1* mutant plants, which have a knock-down mutation of *VPS29* (Supplemental Figure 1). VPS29 is a component of the retromer complex, which mediates protein trafficking from the PVC to the TGN, and localizes to the PVC (Shimada et al., 2006), and defects of VPS29 also affect the morphology of the PVC to give rise to enlarged PVCs. In addition, the defect in the retromer complex suppresses retrograde protein trafficking from the PVC to the TGN and also anterograde trafficking from the TGN to the PVC, thereby affecting turnover of PM proteins (Jaillais et al., 2007). In *mag1-1* plants, sGFP:ABCG25 produced a punctate staining pattern that was similar to that observed upon Wortmannin treatment and accumulated at high levels in the lytic vacuole. Together, these results suggest that sGFP:ABCG25-positive punctate labeling represents the PVC.

ABCG25 Is Internalized from the PM via Clathrin-Mediated Endocytosis and Transported to the Lytic Vacuole

The localization of sGFP:ABCG25 at the PM, PVC, and lytic vacuole raised the possibility that sGFP:ABCG25 is endocytosed from the PM and transported to the vacuole through the PVC. To test this idea, we initially examined the internalization of sGFP:ABCG25 from the PM to endosomes. Clathrin plays a key role in the internalization of PM-localized proteins to endosomes in plants (Chen et al., 2011). The hub domain (HUB) in the C-terminal fragment of clathrin heavy chain inhibits the interaction between clathrin heavy and light chains when expressed at high levels and thereby prevents clathrin triskelion assembly, which in turn results in inhibition of clathrin-mediated endocytosis (Kitakura et al., 2011). We crossed sGFP:ABCG25 plants with HUB:RFP plants or plants harboring the empty vector, and homozygous plants of both crosses were selected at the F2 generation. HUB:RFP was under the control of the 4-hydroxytamoxifen-inducible promoter (Kitakura et al., 2011). To induce expression of *HUB:RFP*, plants were treated with 4-hydroxytamoxifen for 48 h. HUB:RFP was readily detected in the cytosol and also at the PM, whereas control plants harboring the empty vector did not show any red signals (Figure 3A), confirming that the red signals represent HUB:RFP. Transgenic plants harboring *sGFP:ABCG25* together with *HUB:RFP* or the empty vector were treated with 4-hydroxytamoxifen, and internalization of sGFP:ABCG25 was examined. Upon expression of *HUB:RFP*, sGFP:ABCG25 produced a strong PM pattern together with fewer puncta, compared with control plants harboring the empty vector (Figure 3A). To confirm that fewer puncta were caused by inhibition of endocytosis, we examined the accumulation of sGFP:ABCG25 at the BFA body after BFA treatment. GFP signals at BFA bodies were significantly lower in plants expressing HUB:RFP than in control plants (Figure 3A; Supplemental Figure 2). To obtain supporting evidence for this, we

examined the effect of Tyrphostin A23 (Tyr A23) on the internalization of sGFP:ABCG25. Tyr A23 strongly inhibits clathrin-mediated endocytosis in plants (Dhonukshe et al., 2007). Tyr A23 treatment significantly reduced GFP signals at the punctate labeling and at BFA bodies upon BFA treatment (Figures 3B and 3C). In these experiments, CHX was included in the treatment to eliminate the accumulation of newly synthesized sGFP:ABCG25 at endosomes. Together, these results suggest that sGFP:ABCG25 is internalized from the PM to endosomes via clathrin-mediated endocytosis.

Clathrin-dependent endocytosis of sGFP:ABCG25 prompted us to examine whether endocytosis of sGFP:ABCG25 is dependent on the heterotetrameric adaptor protein complex 2 (AP-2). AP-2 functions as an adaptor of clathrin-mediated endocytosis (Di Rubbo et al., 2013; Kim et al., 2013; Yamaoka et al., 2013). sGFP:ABCG25 plants were crossed with *ap2m* mutant plants that have a mutation in the medium subunit of AP-2. The signal intensity at the BFA body is a convenient way to assess the rate of endocytosis (Geldner et al., 2003). We examined BFA body formation in root cells in a time-dependent manner. In wild-type plants, sGFP:ABCG25 started to accumulate at the BFA body at 10 min after BFA treatment and continued to increase throughout the observation period (30 min). By contrast, sGFP:ABCG25 was hardly detected at the BFA body in *ap2m* mutant plants even at 40 min after BFA treatment (Figure 3D), indicating that AP-2 is involved in endocytosis of sGFP:ABCG25. Moreover, this result supports the idea that sGFP:ABCG25 is internalized via clathrin-mediated endocytosis.

Exogenously Applied ABA Increases sGFP:ABCG25 Levels at the PM by Enhancing Recycling from Endosomes

In plants, the cellular ABA levels are regulated depending on the plant growth stage and environmental conditions. We examined whether high levels of ABA affect the subcellular localization of ABCG25. sGFP:ABCG25 seedlings vertically grown on solid 0.5× Murashige and Skoog (MS) plates were transferred to MS liquid medium supplemented with ABA or DMSO, and the localization of sGFP:ABCG25 was examined. DMSO was used as the solvent for ABA. After incubation for 4 h, sGFP:ABCG25 signals at the PM were greatly decreased in DMSO-containing medium but maintained at high levels in ABA-containing medium (Figure 4A), indicating that sGFP:ABCG25 levels at the PM were affected by exogenously applied ABA. One possible explanation for the difference in GFP signals between DMSO- and ABA-containing media is that sGFP:ABCG25 is degraded in DMSO-containing medium, but exogenously applied ABA can block the turnover of sGFP:ABCG25, thereby leading to its accumulation at the PM at high levels. High levels of ABA may inhibit endocytosis of sGFP:ABCG25. This may be opposite to enhanced endocytosis under high osmotic stress conditions (Martinière et al., 2012). To test this idea, we examined sGFP:ABCG25 levels after BFA treatment. In

Figure 1. (continued).

(F) and **(G)** Localization of sGFP:ABCG25 in lytic vacuoles. Five-day-old seedlings were treated with Con A (2 μM) for 4 h or incubated in darkness for 6 h. Bars = 10 μm.
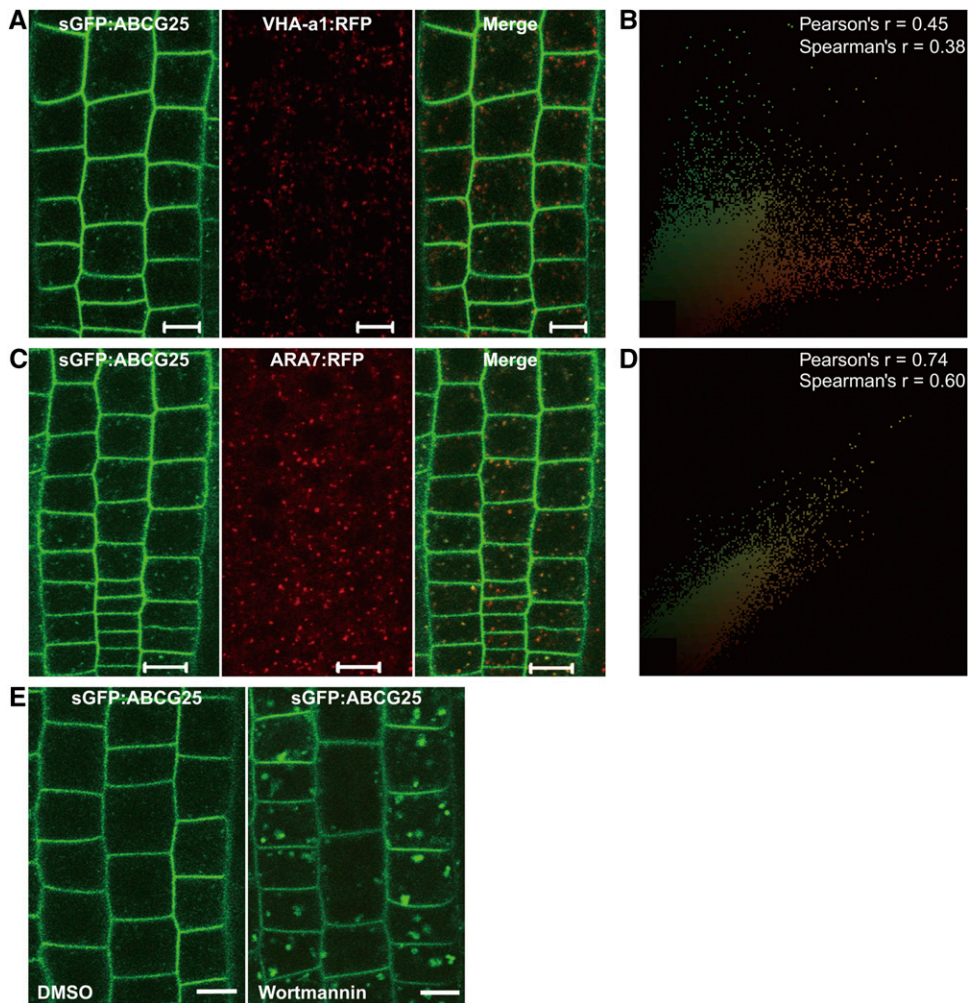
Figure 2. sGFP:ABCG25-Positive Endosomes Are Transported to the Lytic Vacuole via the PVC in Normal Growth Conditions.

(A) to **(D)** Colocalization of sGFP:ABCG25 with ARA7:RFP, but not with VHA-a1:RFP, in root tip cells. Transgenic plants harboring *sGFP:ABCG25* together with *VHA-a1:RFP* **(A)** or *ARA7:RFP* **(C)** were examined for colocalization of sGFP:ABCG25 with VHA-a1 or ARA7 using a CLSM. Green, sGFP:ABCG25; red, ARA7:RFP or VHA-a1:RFP. Bars = 10 μm.

(B) and **(D)** The extent of the colocalization of green and red fluorescent signals was analyzed by ImageJ to obtain Pearson-Spearman correlation coefficients. The resulting scatterplots are shown along with r_p and r_s values. The level of colocalization ranged from +1 (complete colocalization) to −1 (no correlation). Analysis of the colocalization between sGFP:ABCG25 and VHA-a1, or between sGFP:ABCG25 and ARA7, was undertaken using 51 and 44 cells, respectively.

(E) Enlargement of sGFP:ABCG25-positive endosomes by Wortmannin treatment. sGFP:ABCG25 plants were treated with Wortmannin (33 μM) for 1.5 h. Bars = 10 μm.

this condition, internalized proteins accumulate at the BFA body and cannot be transported to the vacuole for degradation. In both samples, sGFP:ABCG25 accumulated at the BFA body at similar levels (Figure 4B). Indeed, the ratios of GFP signals between the cytosol and PM were nearly the same in both samples (Figure 4C), indicating that endocytosis of sGFP:ABCG25 occurs at the same rate in DMSO- and ABA-containing media.

To further examine how plant cells maintain high levels of sGFP:ABCG25 at the PM in ABA-containing medium, we examined the rate of recycling from endosomes to the PM. At endosomes, endocytosed proteins can be either targeted to the vacuole for degradation or recycled back to the PM. To measure the rate of recycling from endosomes to the PM, we measured the rate of GFP signal disappearance from the BFA body after washing out BFA from the cell in a time-dependent manner (Figure 4D). sGFP:ABCG25 seedlings treated with BFA for 1 h were transferred to ABA- or DMSO-containing liquid media, and GFP signals were observed at 1 or 2 h after transfer. At 1 h after transfer to DMSO- or ABA-containing media, GFP signals were diminished at the BFA body in both cases. The rate of disappearance of GFP signals from the BFA body was more rapid in ABA-containing medium than in DMSO-containing medium; concomitantly, GFP signals at the PM were stronger in ABA-containing medium than in DMSO-containing medium. Finally, at 2 h after transfer to ABA-containing
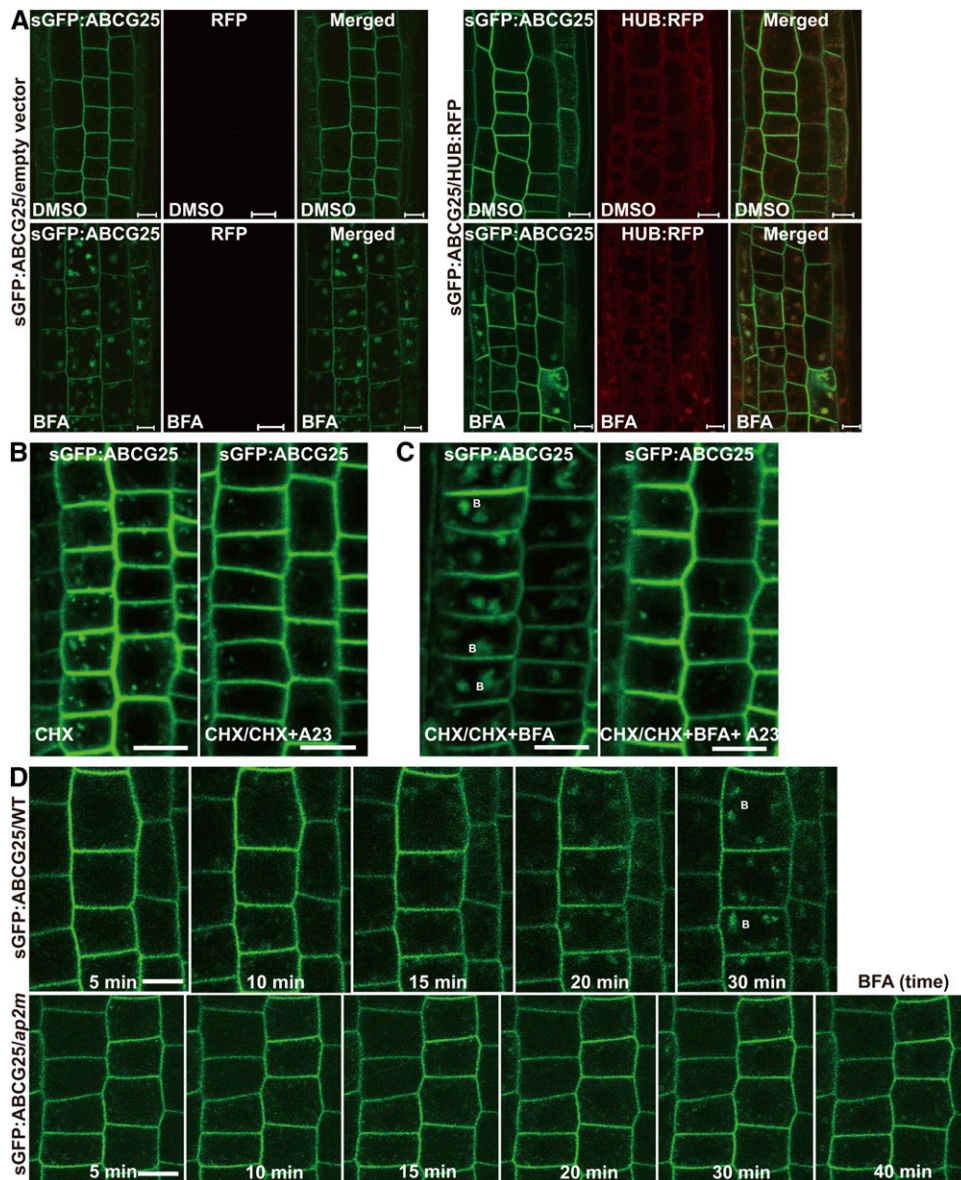
Figure 3. Clathrin and AP-2 Are Involved in Internalization of sGFP:ABCG25 from the PM to Endosomes.

(A) Effect of HUB:RFP on the internalization of sGFP:ABCG25. Transgenic plants harboring *sGFP:ABCG25* together with *HUB:RFP* or the empty vector as a control were grown on 0.5× MS plates for 5 d and transferred to 2 μM 4-hydroxytamoxifen-containing liquid medium for 48 h. The localization of sGFP: ABCG25 was examined in the presence of DMSO and 50 μM BFA. Bars = 10 μm.
(B) Inhibition of sGFP:ABCG25 internalization by Tyr A23. Five-day-old sGFP:ABCG25 seedlings that had been treated with 50 μM CHX for 1 h were treated with 30 μM Tyr A23 (A23) for 30 min, and the localization of sGFP:ABCG25 was examined in epidermal and cortex cells of root tips. Bars = 10 μm.
(C) Accumulation of sGFP:ABCG25 at the BFA body. sGFP:ABCG25 seedlings (5 d old) were treated with 50 μM BFA alone or together with 30 μM Tyr A23, and the localization of sGFP:ABCG25 was examined. Bars = 10 μm.
(D) Internalization of sGFP:ABCG25 to the BFA body in *ap2m* plants. Wild-type and *ap2m* mutant plants expressing *sGFP:ABCG25* were treated with BFA (50 μM). The accumulation of sGFP:ABCG25 at the BFA body was compared between wild-type and *ap2m* plants at various time points. B, BFA body. Bars = 10 μm.

media, GFP signals at the BFA body had almost completely disappeared and concomitantly GFP signals were increased at the PM but not in the lytic vacuole, indicating that high levels of ABA enhance recycling of sGFP:ABCG25 from endosomal compartments to the PM. By contrast, in DMSO-containing medium, GFP signals were significantly increased in lytic vacuoles with the

concomitant disappearance of GFP signals from the BFA body, indicating that a large proportion of sGFP:ABCG25 traffics to the lytic vacuole in addition to trafficking to the PM in DMSO-containing medium. To assess the enhancement of recycling, the ratio of cytosolic GFP signals, including that at BFA bodies, to GFP signals at the PM was determined at 1 h after transfer. The ratio was 10% lower
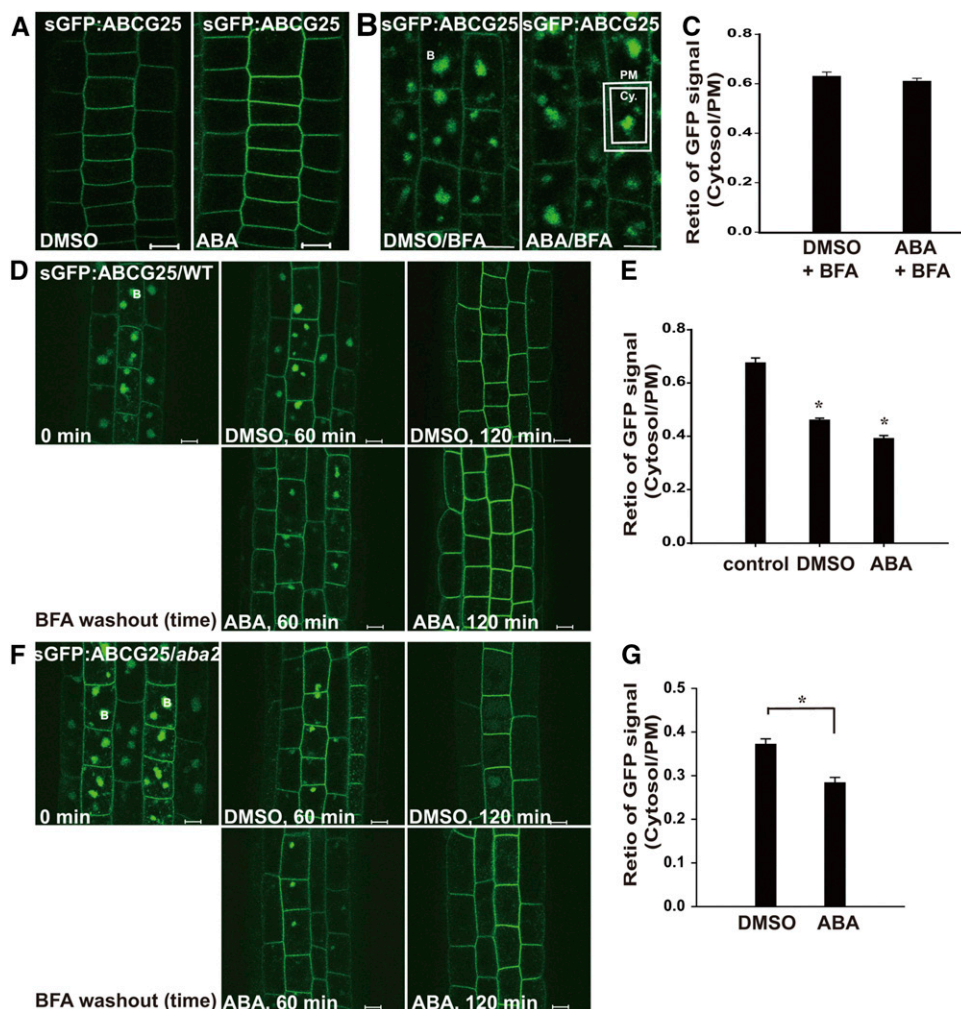
Figure 4. Application of Exogenous ABA Enhances Recycling of sGFP:ABCG25 from Endosomes to the PM.

(A) and **(B)** Effect of exogenous ABA on the levels of sGFP:ABCG25.

(A) sGFP:ABCG25 plants (5 d old) were incubated in DMSO- or ABA (10 μM)-containing 0.5× MS media for 4 h, and the sGFP:ABCG25 signal intensity was examined.

(B) Five-day-old sGFP:ABCG25 seedlings that had been incubated in DMSO- or 10 μM ABA-containing 0.5× MS media were treated with 50 μM BFA for 30 min. The PM and cytosolic areas are indicated by dotted lines. B, BFA body. Bar = 10 μm.

(C) Quantification of the relative GFP signal intensity between the cytosol and PM. GFP signals marked as the PM and cytosol in **(B)** were measured separately and used to calculate the ratio of the signal intensity between cytosolic and PM-localized sGFP:ABCG25 proteins. Error bars indicate sd; the cell number (n) = 20.

(D) and **(F)** Effect of exogenously applied ABA on recycling of sGFP:ABCG25 from the BFA body to the PM.

(D) Plants that had been treated with 50 μM BFA for 1 h were transferred to 0.5× MS liquid media containing DMSO or 10 μM ABA. The localization of sGFP:ABCG25 was examined at 1 or 2 h. Bar = 10 μm.

(E) The relative GFP signal intensity between the cytosol and PM in **(D)** was quantified as in **(C)**. Asterisks mark significant differences (Student's t test, $P <$ 0.05). Error bars indicate sd; the number of cells (n) = 17.

(F) and **(G)** The effect of exogenously applied ABA on the recycling of sGFP:ABCG25 in *aba2* plants.

(F) Five-day-old seedlings that had been treated with 50 μM BFA for 1 h were transferred to 0.5× MS liquid medium containing DMSO or 10 μM ABA. The disappearance of sGFP:ABCG25 from the BFA body was measured at the indicated time points. An enlarged image of single root cells is shown on the right side. B, BFA body; V, vacuole. Bars = 10 μm.

(G) The relative GFP signal intensity between the cytosol and PM in **(F)** was quantified at the 2-h time point as in **(C)**. Asterisks indicate significant differences (Student's t test, $P <$ 0.05). Error bars indicate sd; the number of cells (n) = 24.

in ABA-containing medium than in DMSO-containing medium (Figure 4E). In addition, we examined the kinetics of the effect of ABA on recycling of sGFP:ABCG25. Disappearance of sGFP:ABCG25 from the BFA bodies in the presence of ABA was faster than in the presence of DMSO (control) (Supplemental Figure 3). To further confirm that ABA levels are important for the recycling of ABCG25, we introduced *sGFP:ABCG25* into *aba2-1* mutant plants. ABA2 is a key enzyme involved in de novo ABA biosynthesis (González-

Guzmán et al., 2002). Thus, *aba2-1* mutant plants with a point mutation in ABA2 show severely reduced production of ABA. The disappearance of ABCG25 from the BFA body in the *aba2* background was similar to that in the wild-type background at the 1-h time point. However, ABCG25 was strongly detected at lytic vacuoles at 2 h after washout in the DMSO control, whereas exogenous ABA treatment inhibited vacuolar targeting of ABCG25 and increased GFP signal at the PM (Figures 4F and 4G). Together, these results suggest that high levels of ABA facilitate recycling of sGFP:ABCG25 from endosomes to the PM.

Recycling of ABCG25 Is Impaired in the ABA-Insensitive Mutant

To gain insight into the mechanism by which high levels of ABA enhance recycling of sGFP:ABCG25, we examined if recycling of sGFP:ABCG25 involves ABA-mediated signaling. ABA signaling is initiated by binding of ABA to ABA receptors, pyrabactin resistance (PYR)/PYR1-like (PYL)/Regulatory Component of Abscisic acid Receptor (RCAR), which are START domain-containing proteins (Ma et al., 2009; Park et al., 2009). The ABA receptors are encoded by 14 genes, *PYR1* and *PYL1* to *13* in Arabidopsis (Ma et al., 2009; Park et al., 2009). *pyr1 pyl1 pyl2 pyl4* quadruple mutant plants (QC3 plants) show a strong ABA-insensitive phenotype in diverse ABA responses, in particular, a severe defect in the expression of ABA-responsive genes (Park et al., 2009). We compared the subcellular localization of sGFP:ABCG25 between wild-type and QC3 plants and found that more speckles were produced in QC3 plants than in wild-type plants (Figure 5A). To elucidate the underlying cause of difference in ABCG25 localization between wild-type and QC3 plants, we first tested whether these plants have any difference in endogenous ABA levels. We measured ABA levels in 2-week-old wild-type and QC3 plants. Wild-type and QC3 plants showed similar levels of ABA to each other (5.1 ng/g $\pm$ 0.8 in wild-type plants and 6.5 ng/g $\pm$ 1.1 in QC3 plants; $n = 6$ with SD), indicating that the difference in ABCG25 localization between wild-type and QC3 plants is not due to the difference in ABA levels. Next, we examined the involvement of cytosolic ABA signaling in the subcellular localization of sGFP:ABCG25. Again, we performed the BFA washout experiment using sGFP:ABCG25 in root tissues of QC3 plants. At 1 h after BFA treatment (0 time point for BFA washout), the levels of sGFP:ABCG25 accumulated at the BFA body in QC3 plants were comparable to those in wild-type plants (Figure 5B), indicating that the endocytosis rate of sGFP:ABCG25 was not affected in QC3 plants. However, in the presence of ABA, the disappearance of sGFP:ABCG25 from the BFA body was significantly slower in QC3 plants than in wild-type plants after BFA washout. In QC3 plants, GFP signals were still strongly detected at BFA bodies under both the DMSO and ABA treatments even at 2 h after BFA washout. At this time point, GFP signals had almost completely disappeared in both DMSO and ABA-treated wild-type plants (Figure 4D). These results indicate that cytosolic ABA signaling plays a key role in the recycling of sGFP:ABCG25 from endosomes to the PM. As a control, we examined the behavior of a GFP fusion of another PM protein, PIN2:GFP, under the same conditions. Endocytosis and recycling of PIN proteins are well characterized at the molecular and cellular levels (Dhonukshe
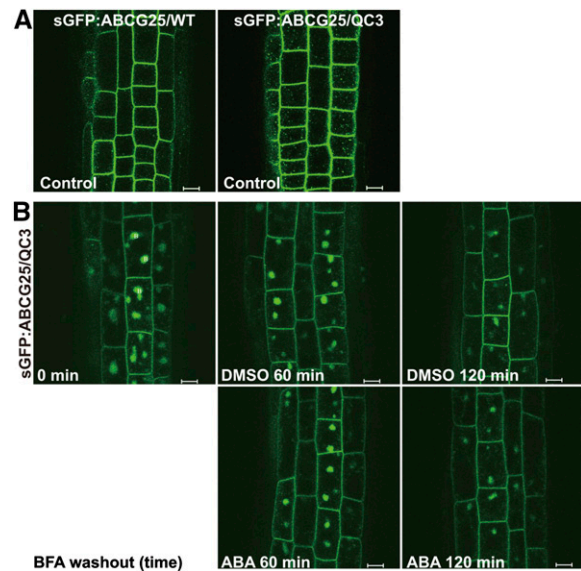

Figure 5. ABA-Induced Recycling of sGFP:ABCG25 from Endosomes to the PM Is Defective in ABA-Insensitive Mutant Plants.

(A) The levels of PM-localized sGFP:ABCG25 in QC3 mutant plants. Wild-type and QC3 seedlings harboring *sGFP:ABCG25* were grown on 0.5× MS plates for 5 d, and GFP signals were examined in root tip cells. Bars = 10 μm.
(B) The effect of exogenously applied ABA on the recycling of sGFP:ABCG25 in QC3 plants. Five-day-old seedlings that had been treated with 50 μM BFA for 1 h were transferred to 0.5× MS liquid medium containing DMSO or 10 μM ABA. The disappearance of sGFP:ABCG25 from the BFA body was measured at the indicated time points. B, BFA body. Bars = 10 μm.

et al., 2007; Kitakura et al., 2011; Di Rubbo et al., 2013; Geldner et al., 2001; Kleine-Vehn et al., 2011). The rate of PIN2:GFP recycling from BFA bodies to the PM after BFA washout was not affected by exogenously applied ABA (Supplemental Figure 4), indicating that the effect of ABA on recycling of proteins from endosomes to the PM is specific to sGFP:ABCG25.

Next, we examined the recycling pathway of sGFP:ABCG25 in the presence of ABA in the incubation medium. Endocytosed proteins are generally recycled from the TGN/EE to the PM (Luschnig and Vert, 2014). We examined the localization of sGFP:ABCG25 in *mag1-1* plants in ABA- or DMSO-containing media (Supplemental Figure 5). *mag1-1* plants have a defect in retrograde trafficking from the PVC to the TGN (Nodzynski et al., 2013). sGFP:ABCG25 localized to multiple endosomal organelles in addition to the PM in the presence of DMSO. Upon ABA treatment, the endosomal signal intensity was reduced and the PM signals were concomitantly increased (Supplemental Figure 5), indicating that ABA-induced recycling of sGFP:ABCG25 from endosomes to the PM occurs normally in *mag1-1* plants. These results suggest that the recycling of sGFP:ABCG25 occurs at the TGN/EE.

Abiotic Stress Enhances Internalization of ABCG25 from the PM to Endosomes

The effect of exogenously applied ABA on the localization of sGFP:ABCG25 prompted us to examine the possibility that various abiotic stresses also influence the localization of sGFP:ABCG25.

sGFP:ABCG25 plants were incubated with NaCl or polyethylene glycol (PEG), and the localization of sGFP:ABCG25 was examined. These plants were also stained with FM4-64 for a short period of time prior to examining the localization of sGFP: ABCG25. After 3 h of treatment with NaCl or PEG, GFP signals were greatly increased at the lytic vacuole, compared with control conditions (Figures 6A to 6C). In these conditions, FM4-64 largely localized to endosomes, indicating that vacuolar trafficking of sGFP:ABCG25 was accelerated compared with that of FM4-64. We examined whether endocytosis of sGFP:ABCG25 was enhanced under high NaCl conditions. sGFP:ABCG25 seedlings were treated with or without NaCl for 1 h in the presence of BFA, and the signal intensity of sGFP:ABCG25 at the BFA body was compared between NaCl-treated and control plants. GFP signals at the BFA body were significantly stronger in NaCl-treated plants than in control plants (Figure 6D), indicating that NaCl stress facilitates endocytosis of sGFP:ABCG25. To assess the degree of enhanced endocytosis, we quantified GFP signals in the cytosol and PM before and after NaCl treatment in the presence of BFA. The ratio of cytosolic to PM GFP signals was 20% higher upon NaCl treatment (Figure 6E). To confirm the effect of NaCl stress on the internalization of sGFP:ABCG25, we examined the kinetics of sGFP:ABCG25 endocytosis. At early time points (10 and 20 min) after NaCl treatment, endosomes showing GFP signals were rarely observed in either control or NaCl-treated samples, indicating no significant difference in the endocytosis of sGFP: ABCG25 between the two (Supplemental Figure 6). However, 40 min after NaCl treatment, the number of endosomes showing GFP signals and the intensity of the signals in the endosome gradually increased when compared with the control samples. These results suggest that various abiotic stresses activate endocytosis of ABCG25 from the PM to prevent ABA efflux and increase cytosolic ABA levels. Moreover, the strong GFP signals in the vacuole suggest that internalized sGFP:ABCG25 is transported to the vacuole for degradation. Because *ABCG25* is predominantly expressed in the phloem companion cells in root tissues (Kuromori et al., 2014), we investigated whether this type of regulation also occurs in other types of cells, including the phloem companion cells in the root tissues. We used a multiphoton microscope (MPM) because it has better penetration and resolution. We obtained images of the cells at the cross section of the root tissues using the MPM. However, the companion cells were not easily noticeable in the images. Instead, we found that most of the cells including those at the vascular tissue and endodermal region of the roots showed increases in the number and size of punctate stains upon the NaCl treatment (Figure 7), indicating that salt stress triggers endocytosis of ABCG25 in the cells of the root tissues regardless of the cell type.

Next, we asked whether clathrin is involved in NaCl-induced endocytosis of sGFP:ABCG25. Transgenic plants harboring *sGFP:ABCG25* together with *HUB:RFP* or the empty vector were first treated with 4-hydroxytamoxifen for 48 h and then with NaCl for 1 h, and the localization of sGFP:ABCG25 and expression of HUB:RFP were examined under a microscope. Endocytosis of sGFP:ABCG25 under NaCl stress conditions was strongly inhibited by overexpression of *HUB:RFP* (Figure 6F), indicating that clathrin is involved in NaCl stress-induced endocytosis of sGFP: ABCG25.

Internalization of ABCG25 under Abiotic Stress Is Not Related to ABA Levels or ABA Signaling

To elucidate the mechanism by which NaCl stresses facilitate endocytosis of sGFP:ABCG25, we examined whether ABA is involved in the enhanced endocytosis of sGFP:ABCG25 under abiotic stress conditions. ABA levels are rapidly elevated under abiotic stress conditions to induce various ABA-mediated signaling pathways (Cramer et al., 2011; Xiong et al., 2002). *aba2-1* plants expressing sGFP:ABCG25 were treated with a high concentration of NaCl, and the localization of sGFP:ABCG25 was examined by confocal microscopy. *aba2-1* plants have a defect in the de novo biosynthetic pathway and thus have low levels of ABA and exhibit defects in abiotic stress responses. Upon treatment with a high concentration of NaCl, sGFP:ABCG25 in *aba2-1* plants, similar to wild-type plants, showed strong punctate staining and vacuolar GFP patterns (Figure 8A), indicating that the defect in de novo biosynthesis of ABA does not affect the enhanced endocytosis of sGFP:ABCG25 induced by NaCl stress. This indicates that higher levels of ABA are not required for endocytosis of ABCG25.

Next, we examined whether endocytosis of sGFP:ABCG25 is regulated by ABA signaling. Under NaCl stress conditions, we again examined endocytosis of sGFP:ABCG25 in QC3 plants. QC3 plants have a defect in ABA signaling and thus exhibit ABA insensitivity. Even in the absence of NaCl stress, QC3 plants produced a strong punctate staining pattern that was stronger than that in wild-type plants (Figure 8B), raising the possibility that endocytosis of sGFP:ABCG25 occurs normally in QC3 plants. Under high NaCl stress conditions, QC3 plants showed strong vacuolar GFP signals that were comparable to those in wild-type plants, confirming that endocytosis of sGFP:ABCG25 was not affected in QC3 plants. These results suggest that ABA-mediated signaling is not involved in endocytosis of sGFP:ABCG25.

DISCUSSION

sGFP:ABCG25 Is Internalized from the PM via Endocytosis and Transported to the Lytic Vacuole for Degradation

In this study, we provide compelling evidence that ABCG25 is subject to posttranslational regulation via endocytosis followed by trafficking to the vacuole via the PVC. Recently, in plants, clathrin-mediated endocytosis has been implicated in the regulation of many PM-localized proteins, such as pattern recognition receptors involved in defense responses and ion transporters (Robatzek et al., 2006; Wang et al., 2013). Similar to these proteins, endocytosis of sGFP:ABCG25 was also mediated by clathrin, as evidenced by the fact that it was inhibited by overexpression of HUB:RFP and in *ap2m* plants. The clathrin light chain binds to the C-terminal domain (named HUB) of the clathrin heavy chain. Overexpression of HUB leads to inhibition of clathrin-coated vesicle formation and thereby inhibits endocytosis. Thus, RFP-fused HUB expressed in HUB:RFP transgenic plants by treating with 4-hydroxytamoxifen acts as a dominant negative mutant of the clathrin heavy chain (Kitakura et al., 2011). *ap2m* plants that have a mutation in *AP2M*, which encodes the medium subunit μ-adaptin of heterotetrameric AP-2, display a defect in endocytosis (Di Rubbo
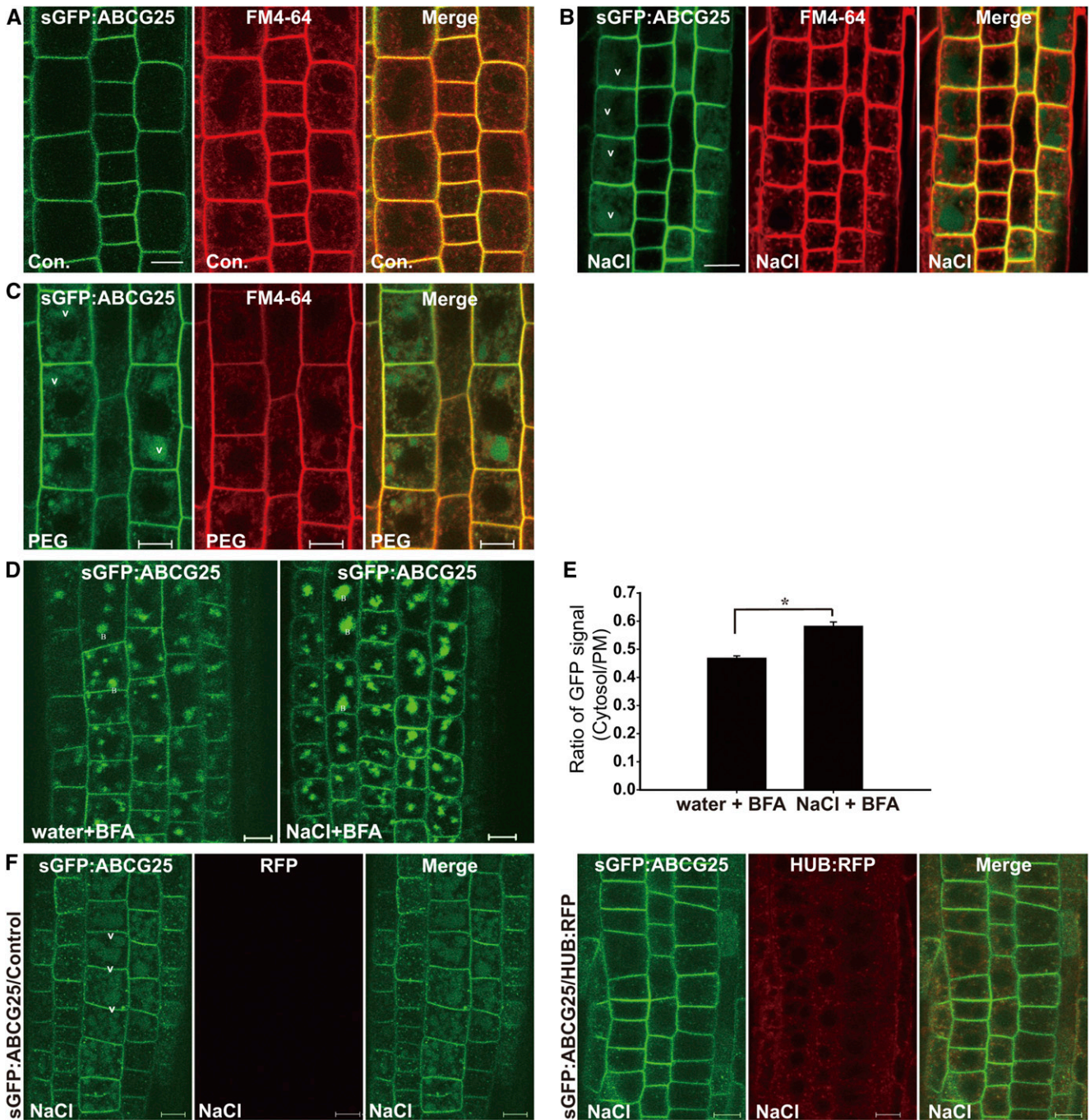
Figure 6. Abiotic Stresses Activate the Internalization of sGFP:ABCG25.

(A) to **(C)** Effects of NaCl and PEG stresses on the localization of sGFP:ABCG25. Plants grown on 0.5× MS plates for 5 d were further incubated for 3 h in normal 0.5× MS medium **(A)** or 0.5× MS medium containing 100 mM NaCl **(B)** or 20% (w/v) PEG 8000 **(C)**. All plants were stained with FM4-64, and the localizations of sGFP:ABCG25 and FM4-64 were examined. V, vacuole. Bars = 10 μm.

(D) and **(E)** Effect of a high NaCl concentration on the endocytosis of sGFP:ABCG25.

(D) Plants were simultaneously treated with BFA with or without 100 mM NaCl for 1 h, and the localization of sGFP:ABCG25 was examined.

(E) Quantification of the endocytosis rate. To quantify the increase in the endocytosis rate caused by exposure to a high concentration of NaCl, the signal intensities of cytosolic and PM-localized sGFP:ABCG25 in **(D)** were measured separately and their relative ratio was calculated. Error bars indicate sD; the number of cells (*n*) = 31. The asterisk marks a significant difference (Student's *t* test, P < 0.05). B, BFA body; V, vacuole. Bars = 10 μm.
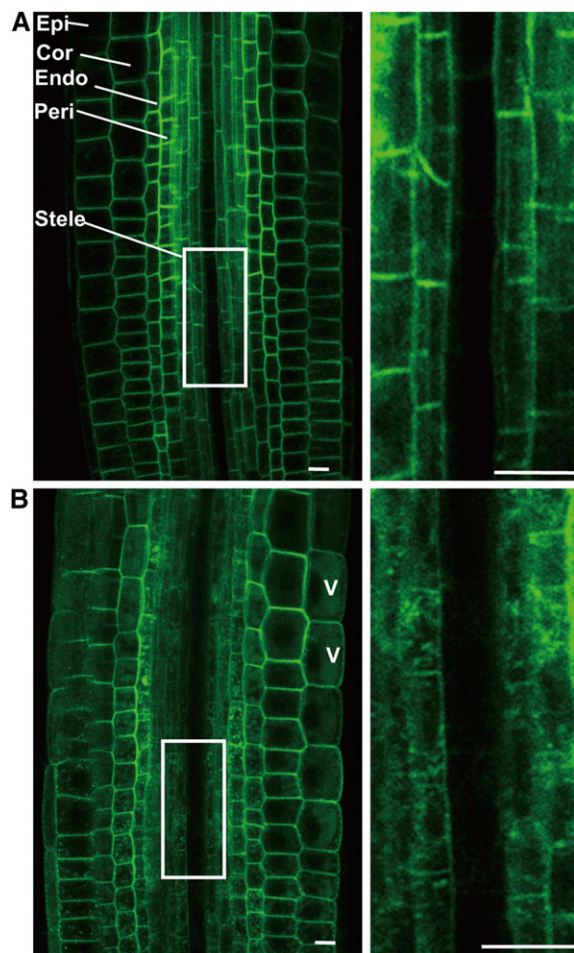
Figure 7. Salt Stress-Induced Endocytosis of sGFP:ABCG25 Occurs in Various Root Cells, Independent of Cell Type.

Multiphoton microscopy was used to examine the effect of salt stress on the endocytosis of ABCG25 in various types of root cell. Five-day-old seedlings harboring *sGFP:ABCG25* were treated with water **(A)** or 100 mM NaCl **(B)** for 90 min. Images were acquired by focusing on the center of the root. Images of a single focal plane are shown. Right panels show magnified images of the boxed areas in the left panels. Epi, epidermis; Cor, cortex; Endo, endodermis; Peri, pericycle; V, vacuole. Bars = 10 μm.

et al., 2013; Kim et al., 2013; Yamaoka et al., 2013). Thus, ABCG25 is a member of a growing family of proteins whose activity is regulated via endocytosis in plants. In line with this finding, the involvement of clathrin in ABA-mediated processes was reported previously; plants with mutations in clathrin heavy chain display an ABA-hyposensitive phenotype in postgerminative growth (Kansup et al., 2013). However, it should be noted that mutations in the genes encoding

subunits of AP-2 and clathrin coat proteins cause pleiotropic phenotypes due to defects in endocytosis of many cargo proteins (Kitakura et al., 2011; Di Rubbo et al., 2013; Kim et al., 2013; Yamaoka et al., 2013). Thus, clathrin-mediated endocytosis of ABCG25 followed by trafficking to the vacuole through the PVC is a mechanism to regulate the levels of ABCG25 at the PM.

The Spatial Localization of ABCG25 Is Regulated under Various Abiotic Conditions and by the Cellular ABA Levels

ABCG25 pumps out ABA from the cytosol to the apoplast, which implies that proper levels of PM-localized ABCG25 are critical for regulating the cellular ABA levels. Under abiotic stress conditions, plant cells need to increase the cellular ABA levels to induce ABA-mediated signaling in order to respond to abiotic stresses (Cramer et al., 2011; Xiong et al., 2002). Under abiotic stress conditions, biosynthetic genes are expressed at higher levels to increase the cellular ABA levels (Cheng et al., 2002; Iuchi et al., 2001; Seo et al., 2000; Xiong et al., 2001, 2002). In this condition, low levels of ABCG25 at the PM would contribute to the rapid increase of the cellular ABA levels. Consistent with this idea, under abiotic stress conditions, the level of sGFP:ABCG25 at the PM was decreased and concomitantly the levels of sGFP:ABCG25 at endosomes and lytic vacuoles were increased. The lower sGFP:ABCG25 level at the PM was achieved by activation of endocytosis followed by trafficking to the vacuole. Thus, our study provides evidence that removal of PM-localized ABCG25 via activation of endocytosis and transport to the vacuole is another mechanism by which plant cells increase cellular ABA levels under abiotic stress conditions, in addition to the activation of ABA biosynthetic genes. In this process, the activation of ABCG25 endocytosis under abiotic stress conditions occurs in an ABA-independent manner; NaCl stress activates sGFP:ABCG25 endocytosis in both *aba2-1* and QC3 plants, as it does in wild-type plants. Currently, it is not known how endocytosis of sGFP:ABCG25 is activated under abiotic stress conditions. Recent studies showed that many PM-localized proteins such as PIN2 and plasma membrane intrinsic protein 2a (PIP2a) as well as FM4-64 are endocytosed at high rates under abiotic stress conditions (Li et al., 2011; Zwiewka et al., 2015). The exact mechanisms underlying endocytosis activation appear to differ depending on the proteins; in the case of PIN2, endocytosis is enhanced under high NaCl conditions but not under high mannitol conditions (Galvan-Ampudia et al., 2013), whereas sGFP:ABCG25 showed enhanced endocytosis under both high NaCl and PEG conditions.

In plants, high ABA levels attained under abiotic stress conditions need to return to lower levels when conditions return to normal (Wang et al., 2002). Plants contain multiple catabolic pathways to reduce ABA levels (Saito et al., 2004; Dong et al., 2014). In addition, pumping ABA out of the cytosol to apoplasts could contribute to reducing the cellular ABA levels. For this, the levels of ABA exporters need to be increased at the PM.

Figure 6. (continued).

(F) Effect of HUB:RFP on the endocytosis of sGFP:ABCG25 under high NaCl conditions. Five-day-old seedlings harboring *sGFP:ABCG25* together with *HUB:RFP* or the empty vector that had been incubated with 4-hydroxytamoxifen for 2 d were transferred to 0.5× MS liquid media supplemented with or without 100 mM NaCl. The localization of sGFP:ABCG25 and expression of *HUB:RFP* were examined. Bars = 10 μm.
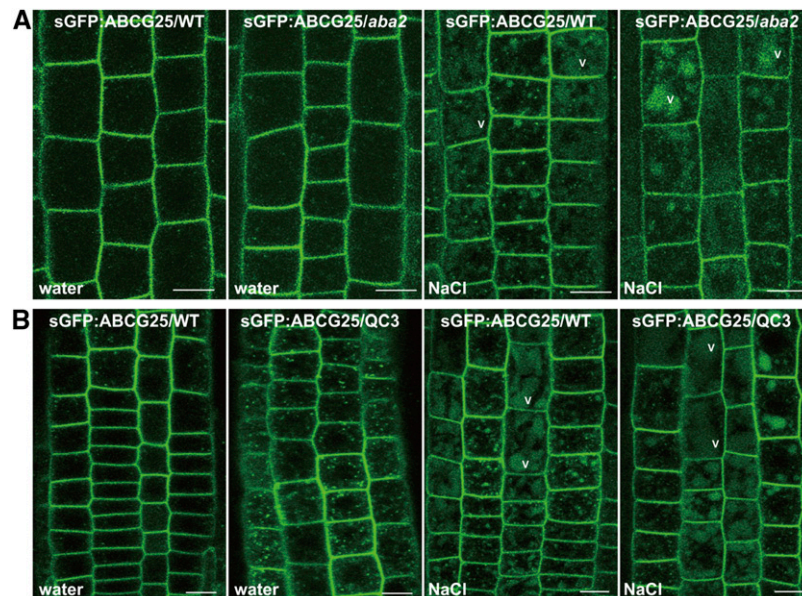
Figure 8. A High Concentration of NaCl Enhances Endocytosis of sGFP:ABCG25 in *aba2* and QC3 Plants.

(A) Effect of NaCl stress on sGFP:ABCG25 endocytosis in *aba2* plants. Both wild-type and *aba2* mutant plants (5 d old) harboring *sGFP:ABCG25* were treated with or without 100 mM NaCl for 3 h, and the localization of sGFP:ABCG25 was examined in root tip cells. Water, no NaCl; V, vacuole. Bars = 10 μm.
(B) Effect of NaCl stress on sGFP:ABCG25 endocytosis in QC3 plans. Both wild-type and QC3 plants (5 d old) harboring sGFP:ABCG25 were treated with or without 100 mM NaCl for 3 h, and the localization of sGFP:ABCG25 was examined in root tip cells. Water, no NaCl; V, vacuole. Bars = 10 μm.

Consistent with this idea, sGFP:ABCG25 levels were higher at the PM upon application of exogenous ABA to plants. The higher levels of sGFP:ABCG25 at the PM can be achieved in two ways: inhibition of endocytosis from the PM to endosomes or enhanced recycling from endosomes to the PM. When ABA levels were high, sGFP:ABCG25 showed enhanced recycling from the BFA body to the PM after BFA washout, whereas the endocytosis rate of sGFP:ABCG25 was not changed. These results suggest that higher levels of sGFP:ABCG25 at the PM are achieved by activation of sGFP:ABCG25 recycling, but not inhibition of endocytosis. The recycling of internalized sGFP:ABCG25 to the PM occurred at the TGN/EE, similar to other plant proteins such as PINs involved in auxin efflux (Tanaka et al., 2014).

One key question is how high levels of ABA activate recycling of ABCG25. In general, when ABA levels are high, ABA binds to ABA receptors to initiate ABA-mediated signaling. Multiple PYR/PYL/RCARs have been identified as cytosolic ABA receptors (Ma et al., 2009; Park et al., 2009). Here, we provide evidence that the cytosolic ABA signaling pathway is crucial for activation of ABCG25 recycling. This conclusion is based on the results showing that ABA-insensitive QC3 plants did not show enhanced sGFP:ABCG25 recycling at high ABA concentrations.

The Contribution of ABCG25 Endocytosis to the Accumulation of ABA in Roots under the Abiotic Stress

Hormones are small signaling mediator molecules whose biosynthesis and working sites are separated from each other. One of the long-standing questions in ABA biology is the long-distance transport of ABA (Zhang and Davies, 1990; Davies et al., 2005).

Transcriptional analysis suggested that ABA is mainly produced in vascular parenchyma cells; ABA biosynthesis genes are actively expressed in these cells in response to abiotic stresses (Endo et al., 2008; Koiwai et al., 2004). Upon exposure to abiotic stresses, high levels of ABA are detected in xylem sap and guard cells, suggesting that ABA biosynthesized in root vascular tissues is transported to guard cells through the transpiration stream (Kuromori and Shinozaki, 2010). However, a recent study showed that guard cells themselves produce ABA within 15 min of exposure to low humidity conditions (Bauer et al., 2013). To directly measure ABA levels in vivo, fluorescence resonance energy transfer-based ABA sensors were recently developed using cytosolic ABA receptors (Waadt et al., 2014). These studies revealed no clear evidence for the long-distance transport of ABA. Geng et al. (2013) also reported that ABA accumulates in both roots and leaves after a 3 h exposure to abiotic stress. However, these reports revealed that accumulation of ABA in root tissues is essential for adaptation to abiotic stress. Indeed, ABA-responsive transcripts are highly increased in the endodermis of roots, promoting lateral root quiescence in response to salt stress (Duan et al., 2013). In this study, we provide evidence that endocytosis of ABCG25 is accelerated in response to salt treatment in the cell of the root division zone. Thus removal of ABCG25 from the PM can contribute to accumulation of ABA in root cells under salt stress (Figures 6 and 7; Supplemental Figure 6). However, we cannot completely rule out the possibility that ABCG25 plays a role in loading of ABA to the phloem. If ABCG25 functions in loading ABA from the biosynthetic sites to the xylem, it would show polar localization at the PM toward the xylem, as do auxin efflux carriers (PINs). However, *sGFP:ABCG25* in transgenic plants showed a uniform distribution to the PM. Of course, this may be due to

overexpression of ABCG25 using the CaMV 35S promoter. Additional ABA exporters may exist in root cells to regulate ABA homeostasis, since ABCG25 is largely expressed in phloem companion cells (Kuromori et al., 2014).

In this study, we showed that salt treatment facilitates endocytosis of ABCG25, whereas ABA treatment induces its localization to the plasma membrane. Thus, the fact that salt treatment, which often induces ABA accumulation (Jia et al., 2002), induces internalization of ABCG25 from the plasma membrane seems to contradict the result showing that exogenous ABA itself has promotes the PM localization of ABCG25. Moreover, the fact that exogenous ABA induces the expression of *ABCG25* (Kuromori et al., 2010, 2014) seems again to contradict the result showing that exogenous ABA induces ABCG25 localization to the PM. It is possible that ABA concentration in the cells determines the localization of ABCG25. ABA levels need to be finely tuned according to the environmental and cellular conditions. ABA levels are increased under abiotic stress conditions such as salt stress. This is achieved by the salt stress-induced expression of ABA biosynthetic genes such as *NCED3* (Barrero et al., 2006). Thus, at the early time points after exposure to salt stress, ABCG25 are rapidly endocytosed to endosomes, thereby contributing to increasing ABA levels within the cell. The high ABA levels activate the adaptation mechanism to salt stress. After the adaptation responses, high ABA levels should be lowered. Indeed, high levels of ABA induce expression of genes encoding ABA catabolic enzymes such as CYP707A1 and ABA UDP-glucosyltransferases (Dong et al., 2014; Saito et al., 2004). Similarly, the high levels of ABA may induce expression of *ABCG25*, which in turn increases ABCG25 levels at the plasma membrane, thereby contributing to lowering the ABA levels. In conclusion, our study suggests that endocytosis is an important mechanism that regulates the activity of ABA transporters, thereby controlling ABA levels in the roots.

Spatial Regulation of ABCG25 as a Component of the Regulatory Mechanism Controlling Cellular ABA Levels

Plants increase ABA levels as a mechanism to respond to abiotic stresses and during embryogenesis. By contrast, ABA levels decrease after responses to abiotic stresses and during germination. Even in a single day, ABA levels fluctuate in a diurnal pattern to respond to changing environmental conditions (Seung et al., 2012). Thus, the cellular ABA levels have to be fine-tuned according to ever-changing environments and the plant growth and developmental stages. The fluctuation of ABA has been studied largely by focusing on two opposing processes, biosynthesis and catabolism of ABA (Seo and Koshiba, 2002). ABA levels are increased via multiple pathways that include de novo biosynthesis in the chloroplast and cytosol, and AtBG1- and AtBG2-mediated hydrolysis of ABA-GE to ABA at the ER and vacuole, respectively (Cheng et al., 2002; Dietz et al., 2000; Endo et al., 2008; Lee et al., 2006; Xu et al., 2012). Also, multiple catabolic pathways exist to reduce ABA levels. These include glucose conjugation of ABA to generate ABA-GE by ABA-UGTs in the cytosol (Dong et al., 2014) and hydroxylation of ABA by cytochrome P450-type CYP707As at the ER surface (Kushiro et al., 2004; Saito et al., 2004). Thus, precise control of the cellular ABA

levels is a highly complicated process involving multiple pathways and multiple organelles. Furthermore, recent findings regarding many transporters including both exporters and importers at the PM add a new layer to the regulation of the cellular ABA levels (Kang et al., 2010; Kanno et al., 2012; Kuromori et al., 2010). One proposed function of ABA exporters and importers is to supply ABA to guard cells in order to regulate stomatal closing (Kang et al., 2010; Kanno et al., 2012; Kuromori et al., 2010). However, here, we provide evidence for a role of ABA exporters in the regulation of cellular ABA levels: they constitute components of the regulatory mechanism by which plant cells control the cellular ABA levels under various cellular and environmental conditions. This is similar to auxin efflux PINs; endocytosis and recycling are involved in the spatial regulation of auxin efflux carriers, PINs, thereby controlling auxin levels to regulate various auxin-related cellular processes (Krecek et al., 2009; Grunewald and Friml, 2010; Löfke et al., 2013).

In summary, our study provides evidence that the spatial regulation of ABCG25 is a component of the mechanism by which plants control cellular ABA levels and also reveals that the mechanism by which ABA levels are fine-tuned according to the environmental and cellular conditions is more complicated than previously appreciated. Moreover, this study raises the question of how plants coordinate all the mechanisms to fine-tune their cellular ABA levels. One possibility is that intricate networks exist to closely coordinate these multiple processes involved in ABA homeostasis according to the cellular and environmental conditions.

METHODS

Plant Growth

Arabidopsis thaliana (ecotype Columbia) was grown on 0.5× MS plates at 23°C in a culture room under a 16-h/8-h light (fluorescent light)/dark cycle. To obtain images of plants, plants were vertically grown for 5 to 6 d on 0.5× MS plates and then transferred to 0.5× MS liquid media for treatment with ABA or other chemicals.

Generation of Transgenic Plants

ABCG25 cDNA was isolated from a cDNA library by PCR using gene-specific primers (Supplemental Table 1). PCR products were inserted into the 326-sGFP vector (Lee et al., 2001) at the C terminus of the sGFP coding sequence. The *sGFP:ABCG25* fusion construct was inserted into the plant binary vector pCsV1300 (Invitrogen), which harbors the cassava vein mosaic virus (CsVMV) promoter, via the *Bam*HI and *Xho*I sites. The binary construct, pCSV1300-sGFP:ABCG25, was introduced into wild-type plants by *Agrobacterium tumefaciens*-mediated floral dipping (Clough and Bent, 1998). Transgenic plants were selected on B5 plates supplemented with hygromycin (25 mg/L).

To introduce *sGFP:ABCG25* into transgenic plants harboring organellar markers, sGFP:ABCG25 plants were crossed with plants harboring *ARA7: RFP* (Lee et al., 2004), *VHA-a1:RFP* (Dettmer et al., 2006), or *HUB:RFP* (Kitakura et al., 2011). Similarly, to introduce sGFP:ABCG25 into various mutant plants, sGFP:ABCG25 plants were crossed with *aba2* (Verslues and Bray, 2006), *ap2m* (Kim et al., 2013), or *mag1-1* (Yamazaki et al., 2008) plants. F1 plants were selected on B5 plates supplemented with hygromycin (25 mg/L), phosphinothricin (25 mg/L), or kanamycin (30 mg/L), and homozygous plants were screened at the F2 generation. To obtain *ap2m* homozygous plants harboring *sGFP:ABCG25*, plants that survived on hygromycin plates were subjected to PCR-mediated genotyping using

ap2m-specific primers (Supplemental Table 1). To obtain *aba2* and *mag1-1* homozygous plants harboring *sGFP:ABCG25*, plants that survived on hygromycin plates were further screened according to phenotypes of *aba2* and *mag1-1*, respectively. To generate QC3 plants harboring *sGFP: ABCG25*, *pCSV1300-sGFP:ABCG25* was transformed into QC3 plants (Gonzalez-Guzman et al., 2012) by Agrobacterium-mediated floral dipping. Transgenic plants were screened on B5 plates supplemented with hygromycin (25 mg/L).

Gene Expression and Phenotype Analysis

To confirm the expression of *sGFP:ABCG25* in transgenic plants, protein extracts were prepared with lysis buffer (100 mM Tris, pH 7.5, 150 mM NaCl, 1 mM EDTA, and 1% Triton X-100) supplemented with an EDTA-free protease inhibitors mixture (Roche Diagnostics). An anti-GFP antibody (mouse, 1:1000; Clontech, cat no. 632381) was used to detect sGFP: ABCG25. Immunoblots were developed using the LAS4000 image capture system (Fujifilm).

To examine the ABA-insensitive phenotype of sGFP:ABCG25 plants, sterilized seeds were planted on 0.5× MS plates containing 1% sucrose in the presence of DMSO or 1 µM ABA. Germination was analyzed based on radicle emergence and green cotyledon development.

Chemical Treatments and in Vivo Imaging

Plants (5- to 6-d-old seedlings) were treated with 2 µM Con A (Invitrogen), 4 µM FM4-64 (Invitrogen), 50 µM CHX (Sigma-Aldrich), 30 µM Tyr A23 (MP-Biomedical), or 33 µM Wortmannin (Enzo Life Science).

For CHX treatment, seedlings were treated with the indicated concentration using 50 mM stock prepared in water for 1 h in liquid 0.5× MS media. For Con A treatment, seedlings were treated with the indicated concentration using 1 mM stock prepared in DMSO for 3 h. For FM4-64 treatment, seedlings were treated at the indicated concentration for 5 min to label endosomes or for 3 h to label the tonoplast. For simultaneous treatment with BFA and FM4-64, BFA was added to the medium for 0.5 h followed by addition of FM4-64. For BFA washout, seedlings that had been treated with BFA for 1 h were transferred to new liquid medium containing DMSO or 10 µM ABA. For Tyr A23 treatment, seedlings were treated with the indicated concentration using 30 mM stock prepared in DMSO for 30 min. For Wortmannin treatment, seedlings were treated with the indicated concentration using 33 mM stock prepared in DMSO for 1.5 h. To apply salinity and osmotic stresses, seedlings grown vertically on 0.5× MS plates were transferred to liquid 0.5× MS media containing 100 mM NaCl or 20% (w/v) PEG 8000 (Ji et al., 2014) for 3 h after FM4-64 staining. To apply dehydration stress, seedlings grown on 0.5× MS plates were exposed to air for 3.5 h by opening the plates. To induce expression of *HUB:RFP*, 5-d-old seedlings were incubated in 0.5× MS liquid media containing 2 µM 4-hydroxytamoxifen for 48 h.

All images of epidermal and cortex cells in the root division zone were acquired using a Zeiss LSM 510 META confocal laser scanning microscope (CLSM), except for the cells of the inner tissues of roots. The filter set had an excitation wavelength/spectral detection bandwidth of 488 nm (argon-ion laser)/515 to 530 nm for GFP, and 458 nm (argon-ion laser)/560 to 615 nm for RFP and FM4-64. All images of control and chemical-treated samples were taken at the exact same settings of the microscope. Images were quantified using ImageJ software (National Institutes of Health). To quantify relative signal intensity, the mean pixel intensity of the cytosolic side and the adjacent PM was measured separately by ImageJ, and the ratios of their values were calculated. To acquire images of cells at the vascular tissues, an MPM with a Ti-Sapphire laser (Chameleon Vision II; Coherent) at 140-fs pulse width and 80-MHz pulse repetition rate was used (TCS SP5 II; Leica). MPM images were acquired and processed by LAS AF Lite (Leica). The filter set had an excitation wavelength/spectral detection bandwidth of 930 nm/500 to 550 nm for GFP.

ABA Quantification by Liquid Chromatography/Mass Spectrometry

Two-week-old seedlings (0.1 to 0.2 g) of Col-0 and QC3 were collected and ground in liquid nitrogen. The metabolites were extracted twice with ethylacetate, and combined extracts were evaporated for 1 h. The residues were dissolved with 70% methanol, vortexed for 10 min, and centrifuged at 15,000 rpm for 10 min at 4°C. The final supernatants were transferred to LC vials (National Scientific Target DP I-D high recovery clear glass vial, flat base, 12 mm diameter × 32 mm height, 1.5 mL) and injected into the liquid chromatography/mass spectrometry system.

UPLC analysis was performed using an ACQUITY UPLC system (Waters) coupled to a QTOF instrument (XEVO G2XS; Waters). Chromatographic separation was performed on an ACQUITY UPLC BEH C18 column (100 × 2.1 mm; i.d., 1.7 µm) connected to an ACQUITY UPLC BEH C18 VanGuard precolumn (5 × 2.1 mm; i.d., 1.7 µm). The mobile phases consisted of 0.1% formic acid and acetonitrile. The gradient elution mode was programmed as follows: 20 to 25% B for 0.0 to 5.0 min and 25 to 35% B for 5.0 to 10.0 min. The column was then washed with 95% B for 3 min and equilibrated with 20% B for 2 min. All samples were kept at 10°C during the analysis. The flow rate and injection volume were 0.4 mL/min and 2 µL, respectively. Mass spectrometry analysis was conducted in negative ion mode with electrospray ionization. The mass spectrometry conditions were optimized as follows: capillary voltage, 3 kV; cone voltage, 40 V; source temperature, 130°C; desolvation temperature, 400°C; cone gas flow, 50 L/h; and desolvation gas flow, 900 L/h.

Accession Numbers

Gene sequences in this article can be found in the Arabidopsis Genome Initiative or GenBank/EMBL databases under the following accession numbers: *AtABCG25*, At1g71960; *AP2M*, At5g46630; *PIN2*, At5g57090; *CLC2*, At2g40060; *ACT2*, At3g18780; *RD29A*, At5g52310; *RD29B*, At5g52300, *NCED3*, At3g14440; *VPS29*, At3g47810; *ARA7*, At4g19640; and *VHA-a1*, At2g28520.

Supplemental Data

Supplemental Figure 1. Subcellular localization of sGFP:ABCG25 in *mag1-1* mutant plants.

Supplemental Figure 2. Accumulation of ABCG25 at BFA bodies is inhibited by HUB.

Supplemental Figure 3. Time-course images of sGFP:ABCG25 after BFA washout in the presence and absence of ABA.

Supplemental Figure 4. Exogenous application of ABA does not affect recycling of PIN2:GFP.

Supplemental Figure 5. *mag1-1* plants do not show any defect in recycling of sGFP:ABCG25.

Supplemental Figure 6. Time-course images of sGFP:ABCG25 during endocytosis in the presence and absence of NaCl stress.

Supplemental Table 1. The nucleotide sequences of primers used in this study.

AUTHOR CONTRIBUTIONS

Y.P., Z.-Y.X., and I.H. conceived the project and designed the research strategies. Y.P. generated most transgenic plants, including sGFP: ABCG25 overexpression lines, and performed most of the imaging-related experiments. Z.-Y.X. generated sGFP:ABCG25 cross lines with ABA-related mutants. S.Y.K. performed MPM observation and some imaging assays. J.L. and B.C. generated sGFP:ABCG25 cross lines with trafficking related mutants and conducted some physiological assays. J.L. performed protein gel blot analysis. H.K. and H.-J.S. measured ABA levels in the wild type and QC3 mutant. Y.P. and I.H. wrote the article.

REFERENCES

Barrero, J.M., Rodríguez, P.L., Quesada, V., Piqueras, P., Ponce, M.R., and Micol, J.L. (2006). Both abscisic acid (ABA)-dependent and ABA-independent pathways govern the induction of NCED3, AAO3 and ABA1 in response to salt stress. Plant Cell Environ. **29:** 2000–2008.

Bauer, H., et al. (2013). The stomatal response to reduced relative humidity requires guard cell-autonomous ABA synthesis. Curr. Biol. **23:** 53–57.

Chen, X., Irani, N.G., and Friml, J. (2011). Clathrin-mediated endocytosis: the gateway into plant cells. Curr. Opin. Plant Biol. **14:** 674–682.

Cheng, W.H., Endo, A., Zhou, L., Penney, J., Chen, H.C., Arroyo, A., Leon, P., Nambara, E., Asami, T., Seo, M., Koshiba, T., and Sheen, J. (2002). A unique short-chain dehydrogenase/reductase in Arabidopsis glucose signaling and abscisic acid biosynthesis and functions. Plant Cell **14:** 2723–2743.

Clough, S.J., and Bent, A.F. (1998). Floral dip: a simplified method for Agrobacterium-mediated transformation of *Arabidopsis thaliana*. Plant J. **16:** 735–743.

Cramer, G.R., Urano, K., Delrot, S., Pezzotti, M., and Shinozaki, K. (2011). Effects of abiotic stress on plants: a systems biology perspective. BMC Plant Biol. **11:** 163.

Davies, W.J., Kudoyarova, G., and Hartung, W. (2005). Long-distance ABA signalling and its relation to other signalling pathways in the detection of soil drying and the mediation of the plant's response to drought. J. Plant Growth Regul. **24:** 285–295.

De Smet, I., Signora, L., Beeckman, T., Inzé, D., Foyer, C.H., and Zhang, H. (2003). An abscisic acid-sensitive checkpoint in lateral root development of Arabidopsis. Plant J. **33:** 543–555.

Dettmer, J., Hong-Hermesdorf, A., Stierhof, Y.D., and Schumacher, K. (2006). Vacuolar H+-ATPase activity is required for endocytic and secretory trafficking in Arabidopsis. Plant Cell **18:** 715–730.

Dhonukshe, P., Aniento, F., Hwang, I., Robinson, D.G., Mravec, J., Stierhof, Y.D., and Friml, J. (2007). Clathrin-mediated constitutive endocytosis of PIN auxin efflux carriers in Arabidopsis. Curr. Biol. **17:** 520–527.

Dietz, K.J., Sauter, A., Wichert, K., Messdaghi, D., and Hartung, W. (2000). Extracellular beta-glucosidase activity in barley involved in the hydrolysis of ABA glucose conjugate in leaves. J. Exp. Bot. **51:** 937–944.

Di Rubbo, S., et al. (2013). The clathrin adaptor complex AP-2 mediates endocytosis of brassinosteroid insensitive1 in Arabidopsis. Plant Cell **25:** 2986–2997.

Dong, T., Xu, Z.Y., Park, Y., Kim, D.H., Lee, Y., and Hwang, I. (2014). Abscisic acid uridine diphosphate glucosyltransferases play a crucial role in abscisic acid homeostasis in Arabidopsis. Plant Physiol. **165:** 277–289.

Duan, L., Dietrich, D., Ng, C.H., Chan, P.M., Bhalerao, R., Bennett, M.J., and Dinneny, J.R. (2013). Endodermal ABA signaling promotes lateral root quiescence during salt stress in Arabidopsis seedlings. Plant Cell **25:** 324–341.

Endo, A., et al. (2008). Drought induction of Arabidopsis 9-cis-epoxycarotenoid dioxygenase occurs in vascular parenchyma cells. Plant Physiol. **147:** 1984–1993.

Galvan-Ampudia, C.S., Julkowska, M.M., Darwish, E., Gandullo, J., Korver, R.A., Brunoud, G., Haring, M.A., Munnik, T., Vernoux, T., and Testerink, C. (2013). Halotropism is a response of plant roots to avoid a saline environment. Curr. Biol. **23:** 2044–2050.

Geldner, N., Anders, N., Wolters, H., Keicher, J., Kornberger, W., Muller, P., Delbarre, A., Ueda, T., Nakano, A., and Jürgens, G. (2003). The Arabidopsis GNOM ARF-GEF mediates endosomal recycling, auxin transport, and auxin-dependent plant growth. Cell **112:** 219–230.

Geldner, N., Friml, J., Stierhof, Y.D., Jurgens, G., and Palme, K. (2001). Auxin transport inhibitors block PIN1 cycling and vesicle trafficking. Nature **413:** 425–428.

Geng, Y., Wu, R., Wee, C.W., Xie, F., Wei, X., Chan, P.M., Tham, C., Duan, L., and Dinneny, J.R. (2013). A spatio-temporal understanding of growth regulation during the salt stress response in Arabidopsis. Plant Cell **25:** 2132–2154.

Gillard, D.F., and Walton, D.C. (1976). Abscisic acid metabolism by a cell-free preparation from *Echinocystis lobata* liquid endoserum. Plant Physiol. **58:** 790–795.

González-Guzmán, M., Apostolova, N., Bellés, J.M., Barrero, J.M., Piqueras, P., Ponce, M.R., Micol, J.L., Serrano, R., and Rodríguez, P.L. (2002). The short-chain alcohol dehydrogenase ABA2 catalyzes the conversion of xanthoxin to abscisic aldehyde. Plant Cell **14:** 1833–1846.

Gonzalez-Guzman, M., Pizzio, G.A., Antoni, R., Vera-Sirera, F., Merilo, E., Bassel, G.W., Fernández, M.A., Holdsworth, M.J., Perez-Amador, M.A., Kollist, H., and Rodriguez, P.L. (2012). Arabidopsis PYR/PYL/RCAR receptors play a major role in quantitative regulation of stomatal aperture and transcriptional response to abscisic acid. Plant Cell **24:** 2483–2496.

Grunewald, W., and Friml, J. (2010). The march of the PINs: developmental plasticity by dynamic polar targeting in plant cells. EMBO J. **29:** 2700–2714.

Iuchi, S., Kobayashi, M., Taji, T., Naramoto, M., Seki, M., Kato, T., and Shinozaki, K. (2001). Regulation of drought tolerance by gene manipulation of 9-cis-epoxycarotenoid dioxygenase, a key enzyme in abscisic acid biosynthesis in Arabidopsis. Plant J. **27:** 325–333.

Iuchi, S., Kobayashi, M., Yamaguchi-Shinozaki, K., and Shinozaki, K. (2000). A stress-inducible gene for 9-cis-epoxycarotenoid dioxygenase involved in abscisic acid biosynthesis under water stress in drought-tolerant cowpea. Plant Physiol. **123:** 553–562.

Jaillais, Y., Santambrogio, M., Rozier, F., Fobis-Loisy, I., Mičge, C., and Gaude, T. (2007). The retromer protein VPS29 links cell polarity and organ initiation in plants. Cell **130:** 1057–1070.

Ji, H., Liu, L., Li, K., Xie, Q., Wang, Z., Zhao, X., and Li, X. (2014). PEG-mediated osmotic stress induces premature differentiation of the root apical meristem and outgrowth of lateral roots in wheat. J. Exp. Bot. **65:** 4863–4872.

Jia, W., Wang, Y., Zhang, S., and Zhang, J. (2002). Salt-stress-induced ABA accumulation is more sensitively triggered in roots than in shoots. J. Exp. Bot. **53:** 2201–2206.

Kang, J., Hwang, J.U., Lee, M., Kim, Y.Y., Assmann, S.M., Martinoia, E., and Lee, Y. (2010). PDR-type ABC transporter mediates cellular uptake of the phytohormone abscisic acid. Proc. Natl. Acad. Sci. USA **107:** 2355–2360.

Kanno, Y., Hanada, A., Chiba, Y., Ichikawa, T., Nakazawa, M., Matsui, M., Koshiba, T., Kamiya, Y., and Seo, M. (2012).

Identification of an abscisic acid transporter by functional screening using the receptor complex as a sensor. Proc. Natl. Acad. Sci. USA **109:** 9653–9658.

Kansup, J., Tsugama, D., Liu, S., and Takano, T. (2013). The Arabidopsis adaptor protein AP-3μ interacts with the G-protein β subunit AGB1 and is involved in abscisic acid regulation of germination and post-germination development. J. Exp. Bot. **64:** 5611–5621.

Kim, S.Y., Xu, Z.Y., Song, K., Kim, D.H., Kang, H., Reichardt, I., Sohn, E.J., Friml, J., Juergens, G., and Hwang, I. (2013). Adaptor protein complex 2-mediated endocytosis is crucial for male reproductive organ development in Arabidopsis. Plant Cell **25:** 2970–2985.

Kitakura, S., Vanneste, S., Robert, S., Löfke, C., Teichmann, T., Tanaka, H., and Friml, J. (2011). Clathrin mediates endocytosis and polar distribution of PIN auxin transporters in Arabidopsis. Plant Cell **23:** 1920–1931.

Kleine-Vehn, J., Leitner, J., Zwiewka, M., Sauer, M., Abas, L., Luschnig, C., and Friml, J. (2008). Differential degradation of PIN2 auxin efflux carrier by retromer-dependent vacuolar targeting. Proc. Natl. Acad. Sci. USA **105:** 17812–17817.

Kleine-Vehn, J., Wabnik, K., Martiniere, A., Langowski, L., Willig, K., Naramoto, S., and Friml, J. (2011). Recycling, clustering, and endocytosis jointly maintain PIN auxin carrier polarity at the plasma membrane. Mol. Syst. Biol. **7:** 540.

Koiwai, H., Nakaminami, K., Seo, M., Mitsuhashi, W., Toyomasu, T., and Koshiba, T. (2004). Tissue-specific localization of an abscisic acid biosynthetic enzyme, AAO3, in Arabidopsis. Plant Physiol. **134:** 1697–1707.

Krecek, P., Skupa, P., Libus, J., Naramoto, S., Tejos, R., Friml, J., and Zazímalová, E. (2009). The PIN-FORMED (PIN) protein family of auxin transporters. Genome Biol. **10:** 249.

Kuromori, T., Miyaji, T., Yabuuchi, H., Shimizu, H., Sugimoto, E., Kamiya, A., Moriyama, Y., and Shinozaki, K. (2010). ABC transporter AtABCG25 is involved in abscisic acid transport and responses. Proc. Natl. Acad. Sci. USA **107:** 2361–2366.

Kuromori, T., and Shinozaki, K. (2010). ABA transport factors found in Arabidopsis ABC transporters. Plant Signal. Behav. **5:** 1124–1126.

Kuromori, T., Sugimoto, E., and Shinozaki, K. (2014). Intertissue signal transfer of abscisic acid from vascular cells to guard cells. Plant Physiol. **164:** 1587–1592.

Kushiro, T., Okamoto, M., Nakabayashi, K., Yamagishi, K., Kitamura, S., Asami, T., Hirai, N., Koshiba, T., Kamiya, Y., and Nambara, E. (2004). The Arabidopsis cytochrome P450 CYP707A encodes ABA 8′-hydroxylases: key enzymes in ABA catabolism. EMBO J. **23:** 1647–1656.

Lee, G.J., Sohn, E.J., Lee, M.H., and Hwang, I. (2004). The Arabidopsis rab5 homologs rha1 and ara7 localize to the prevacuolar compartment. Plant Cell Physiol. **45:** 1211–1220.

Lee, K.H., Piao, H.L., Kim, H.Y., Choi, S.M., Jiang, F., Hartung, W., Hwang, I., Kwak, J.M., Lee, I.J., and Hwang, I. (2006). Activation of glucosidase via stress-induced polymerization rapidly increases active pools of abscisic acid. Cell **126:** 1109–1120.

Lee, Y.J., Kim, D.H., Kim, Y.W., and Hwang, I. (2001). Identification of a signal that distinguishes between the chloroplast outer envelope membrane and the endomembrane system in vivo. Plant Cell **13:** 2175–2190.

Li, X., Wang, X., Yang, Y., Li, R., He, Q., Fang, X., Luu, D.-T., Maurel, C., and Lin, J. (2011). Single-molecule analysis of PIP2;1 dynamics and partitioning reveals multiple modes of Arabidopsis plasma membrane aquaporin regulation. Plant Cell **23:** 3780–3797.

Löfke, C., Luschnig, C., and Kleine-Vehn, J. (2013). Posttranslational modification and trafficking of PIN auxin efflux carriers. Mech. Dev. **130:** 82–94.

Luschnig, C., and Vert, G. (2014). The dynamics of plant plasma membrane proteins: PINs and beyond. Development **141:** 2924–2938.

Ma, Y., Szostkiewicz, I., Korte, A., Moes, D., Yang, Y., Christmann, A., and Grill, E. (2009). Regulators of PP2C phosphatase activity function as abscisic acid sensors. Science **324:** 1064–1068.

Martinière, A., Li, X., Runions, J., Lin, J., Maurel, C., and Luu, D.T. (2012). Salt stress triggers enhanced cycling of Arabidopsis root plasma-membrane aquaporins. Plant Signal. Behav. **7:** 529–532.

Meckel, T., Hurst, A.C., Thiel, G., and Homann, U. (2004). Endocytosis against high turgor: intact guard cells of Vicia faba constitutively endocytose fluorescently labelled plasma membrane and GFP-tagged K-channel KAT1. Plant J. **39:** 182–193.

Nambara, E., and Marion-Poll, A. (2005). Abscisic acid biosynthesis and catabolism. Annu. Rev. Plant Biol. **56:** 165–185.

Nodzynski, T., Feraru, M.I., Hirsch, S., De Rycke, R., Niculaes, C., Boerjan, W., Van Leene, J., De Jaeger, G., Vanneste, S., and Friml, J. (2013). Retromer subunits VPS35A and VPS29 mediate prevacuolar compartment (PVC) function in Arabidopsis. Mol. Plant **6:** 1849–1862.

Park, S.Y., et al. (2009). Abscisic acid inhibits type 2C protein phosphatases via the PYR/PYL family of START proteins. Science **324:** 1068–1071.

Qin, X., and Zeevaart, J.A. (1999). The 9-cis-epoxycarotenoid cleavage reaction is the key regulatory step of abscisic acid biosynthesis in water-stressed bean. Proc. Natl. Acad. Sci. USA **96:** 15354–15361.

Robatzek, S., Chinchilla, D., and Boller, T. (2006). Ligand-induced endocytosis of the pattern recognition receptor FLS2 in Arabidopsis. Genes Dev. **20:** 537–542.

Saito, S., Hirai, N., Matsumoto, C., Ohigashi, H., Ohta, D., Sakata, K., and Mizutani, M. (2004). Arabidopsis CYP707As encode (+)-abscisic acid 8′-hydroxylase, a key enzyme in the oxidative catabolism of abscisic acid. Plant Physiol. **134:** 1439–1449.

Seiler, C., Harshavardhan, V.T., Rajesh, K., Reddy, P.S., Strickert, M., Rolletschek, H., Scholz, U., Wobus, U., and Sreenivasulu, N. (2011). ABA biosynthesis and degradation contributing to ABA homeostasis during barley seed development under control and terminal drought-stress conditions. J. Exp. Bot. **62:** 2615–2632.

Seo, M., and Koshiba, T. (2002). Complex regulation of ABA biosynthesis in plants. Trends Plant Sci. **7:** 41–48.

Seo, M., Peeters, A.J., Koiwai, H., Oritani, T., Marion-Poll, A., Zeevaart, J.A., Koornneef, M., Kamiya, Y., and Koshiba, T. (2000). The Arabidopsis aldehyde oxidase 3 (AAO3) gene product catalyzes the final step in abscisic acid biosynthesis in leaves. Proc. Natl. Acad. Sci. USA **97:** 12908–12913.

Seung, D., Risopatron, J.P., Jones, B.J., and Marc, J. (2012). Circadian clock-dependent gating in ABA signalling networks. Protoplasma **249:** 445–457.

Shimada, T., Koumoto, Y., Li, L., Yamazaki, M., Kondo, M., Nishimura, M., and Hara-Nishimura, I. (2006). AtVPS29, a putative component of a retromer complex, is required for the efficient sorting of seed storage proteins. Plant Cell Physiol. **47:** 1187–1194.

Takano, J., Miwa, K., Yuan, L., von Wirén, N., and Fujiwara, T. (2005). Endocytosis and degradation of BOR1, a boron transporter of *Arabidopsis thaliana*, regulated by boron availability. Proc. Natl. Acad. Sci. USA **102:** 12276–12281.

Tan, B.C., Cline, K., and McCarty, D.R. (2001). Localization and targeting of the VP14 epoxy-carotenoid dioxygenase to chloroplast membranes. Plant J. **27:** 373–382.

Tan, B.C., Joseph, L.M., Deng, W.T., Liu, L., Li, Q.B., Cline, K., and McCarty, D.R. (2003). Molecular characterization of the Arabidopsis 9-cis epoxycarotenoid dioxygenase gene family. Plant J. **35:** 44–56.

Tanaka, H., Nodzyłski, T., Kitakura, S., Feraru, M.I., Sasabe, M., Ishikawa, T., Kleine-Vehn, J., Kakimoto, T., and Friml, J. (2014). BEX1/ARF1A1C is required for BFA-sensitive recycling of PIN auxin transporters and auxin-mediated development in Arabidopsis. Plant Cell Physiol. **55:** 737–749.

Ueda, T., Yamaguchi, M., Uchimiya, H., and Nakano, A. (2001). Ara6, a plant-unique novel type Rab GTPase, functions in the endocytic pathway of *Arabidopsis thaliana*. EMBO J. **20:** 4730–4741.

Verslues, P.E., and Bray, E.A. (2006). Role of abscisic acid (ABA) and Arabidopsis thaliana ABA-insensitive loci in low water potential-induced ABA and proline accumulation. J. Exp. Bot. **57:** 201–212.

Waadt, R., Hitomi, K., Nishimura, N., Hitomi, C., Adams, S.R., Getzoff, E.D., and Schroeder, J.I. (2014). FRET-based reporters for the direct visualization of abscisic acid concentration changes and distribution in Arabidopsis. eLife **3:** e01739.

Wang, Q., Zhao, Y., Luo, W., Li, R., He, Q., Fang, X., Michele, R.D., Ast, C., von Wirén, N., and Lin, J. (2013). Single-particle analysis reveals shutoff control of the Arabidopsis ammonium transporter AMT1;3 by clustering and internalization. Proc. Natl. Acad. Sci. USA **110:** 13204–13209.

Wang, Z., Mambelli, S., and Setter, T.L. (2002). Abscisic acid catabolism in maize kernels in response to water deficit at early endosperm development. Ann. Bot. (Lond.) **90:** 623–630.

Wilkinson, S., and Davies, W.J. (2002). ABA-based chemical signalling: the co-ordination of responses to stress in plants. Plant Cell Environ. **25:** 195–210.

Xiong, L., Ishitani, M., Lee, H., and Zhu, J.K. (2001). The Arabidopsis LOS5/ABA3 locus encodes a molybdenum cofactor sulfurase and modulates cold stress- and osmotic stress-responsive gene expression. Plant Cell **13:** 2063–2083.

Xiong, L., Lee, H., Ishitani, M., and Zhu, J.K. (2002). Regulation of osmotic stress-responsive gene expression by the LOS6/ABA1 locus in Arabidopsis. J. Biol. Chem. **277:** 8588–8596.

Xu, Z.Y., Lee, K.H., Dong, T., Jeong, J.C., Jin, J.B., Kanno, Y., Kim, D.H., Kim, S.Y., Seo, M., Bressan, R.A., Yun, D.J., and Hwang, I. (2012). A vacuolar β-glucosidase homolog that possesses glucose-conjugated abscisic acid hydrolyzing activity plays an important role in osmotic stress responses in Arabidopsis. Plant Cell **24:** 2184–2199.

Yamaoka, S., Shimono, Y., Shirakawa, M., Fukao, Y., Kawase, T., Hatsugai, N., Tamura, K., Shimada, T., and Hara-Nishimura, I. (2013). Identification and dynamics of Arabidopsis adaptor protein-2 complex and its involvement in floral organ development. Plant Cell **25:** 2958–2969.

Yamazaki, M., Shimada, T., Takahashi, H., Tamura, K., Kondo, M., Nishimura, M., and Hara-Nishimura, I. (2008). Arabidopsis VPS35, a retromer component, is required for vacuolar protein sorting and involved in plant growth and leaf senescence. Plant Cell Physiol. **49:** 142–156.

Zhang, J., and Davies, W.J. (1990). Changes of ABA in xylem sap as a function of changing water status can account for changes in leaf conductance and growth. Plant Cell Environ. **13:** 277–285.

Zeevaart, J.A., and Creelman, R.A. (1998). Metabolism and physiology of abscisic acid. Annu. Rev. Plant Physiol. Plant Mol. Biol. **39:** 439–473.

Zhu, J.K. (2002). Salt and drought stress signal transduction in plants. Annu. Rev. Plant Biol. **53:** 247–273.

Zwiewka, M., Nodzyński, T., Robert, S., Vanneste, S., and Friml, J. (2015). Osmotic stress modulates the balance between exocytosis and clathrin-mediated endocytosis in *Arabidopsis thaliana*. Mol. Plant **8:** 1175–1187.

Spatial Regulation of ABCG25, an ABA Exporter, Is an Important Component of the Mechanism Controlling Cellular ABA Levels

Youngmin Park, Zheng-Yi Xu, Soo Youn Kim, Jihyeong Lee, Bongsoo Choi, Juhun Lee, Hyeran Kim, Hee-Jung Sim and Inhwan Hwang

This information is current as of June 20, 2019

Supplemental Data	/content/suppl/2016/09/30/tpc.16.00359.DC1.html
References	This article cites 80 articles, 38 of which can be accessed free at: /content/28/10/2528.full.html#ref-list-1
Permissions	https://www.copyright.com/ccc/openurl.do?sid=pd_hw1532298X&issn=1532298X&WT.mc_id=pd_hw1532298X
eTOCs	Sign up for eTOCs at: http://www.plantcell.org/cgi/alerts/ctmain
CiteTrack Alerts	Sign up for CiteTrack Alerts at: http://www.plantcell.org/cgi/alerts/ctmain
Subscription Information	Subscription Information for *The Plant Cell* and *Plant Physiology* is available at: http://www.aspb.org/publications/subscriptions.cfm